

Review

Metal–Organic Frameworks-Based Analytical Devices for Chiral Sensing and Separations: A Review (2012–2022)

Soodabeh Hassanpour [†], Navid Niaei [†] and Jan Petr ^{*†} 

Department of Analytical Chemistry, Faculty of Science, Palacký University Olomouc, 17. listopadu 12, 77146 Olomouc, Czech Republic

* Correspondence: jan.petr@upol.cz; Tel.: +420-585-63-4416

[†] These authors contributed equally to this work.

Abstract: Metal–organic frameworks (MOFs), as high-surface-area materials, have shown promise in various areas of application, such as chiral sensing and separation, due to their flexibility in design and organized porous cages. Researchers have been striving to design and develop high-performance enantioselective recognition and separation analytical techniques in chiral science fields. The main aim of this review is to provide a comprehensive overview of chirality, state-of-the-art MOFs in chirality, and chiral analysis in the past decade, 2012–2022. The classification of this review includes chirality, principles of chiral analysis, the attraction of functional materials in chirality, MOFs in chiral analysis, MOFs for designing enantioselective sensors (fluorescence, circular dichroism, quartz crystal microbalance, electrochemical), and MOFs as chiral stationary phases (CSPs) for chromatographic enantioseparation (high-performance liquid chromatography, gas chromatography, and capillary electrochromatography). Finally, this review covers the vital progress of these materials with attention to the available opportunities and challenges in this topic.

Keywords: metal–organic frameworks; enantioseparation; enantioselective recognition; chirality; chiral sensing



Citation: Hassanpour, S.; Niaei, N.; Petr, J. Metal–Organic Frameworks-Based Analytical Devices for Chiral Sensing and Separations: A Review (2012–2022). *Chemosensors* **2023**, *11*, 29. <https://doi.org/10.3390/chemosensors11010029>

Academic Editor: Yang Jiao

Received: 7 November 2022

Revised: 23 December 2022

Accepted: 26 December 2022

Published: 29 December 2022



Copyright: © 2022 by the authors. Licensee MDPI, Basel, Switzerland. This article is an open access article distributed under the terms and conditions of the Creative Commons Attribution (CC BY) license (<https://creativecommons.org/licenses/by/4.0/>).

1. Chirality

Chirality is one of the universal and fundamental phenomena in the natural world. It serves a vital role in chemistry, biology, pharmacology, medicine, and food science [1]. The word “chirality” is derived from the Greek word *χειρ* (*kheir*), “hand” in English, and explains the concept that it is impossible to superimpose a molecule onto its mirror image, which is a crucial feature of an asymmetric molecules [2]. Molecular chirality was initially discovered by French scientists Jean-Baptiste Biot and Louis Pasteur in 1848. However, when the “thalidomide disaster” happened in the 1960s, scientists realized the importance of chirality. At present, chirality is considered one of the crucial attributes of a living system, since it is well-known that many “building blocks of life”, such as amino acids, carbohydrates, proteins, and nucleotides, are chiral [2].

Chiral compounds are a pair of a specific type of stereoisomer termed enantiomers or optical isomers (D- and L-forms or R- and S-forms). They are non-superimposable mirror images of each other in 3 dimensions (3D). Although enantiomers possess identical compositions and functional groups, they have distinct, similar, or even reverse biological, pharmacological, and physiological performances in chiral environments, such as the human body, because of various interaction pathways with enzymes or receptors [3,4]. Mainly, a single pure isomer (D-form or L-form) is the active constituent of one molecule and may have desirable features. In contrast, the other isomer may be dysfunctional or exhibit adverse and severe side effects [5]. Most drugs and amino acids (AAs) are generally active in an optically pure form and present as mixtures or racemates with the ineffectual or toxic contrary enantiomer [6]. The enantiomeric purity of various composites has a pivotal role in producing pesticides, food additives, pharmaceuticals, and stereo-specific synthesis.

In contrast, only one of the enantiomers may have satisfactory interaction [7]. Due to their diversity in physiological and pharmacological activities, there is a growing need to separate enantiomeric molecules as single enantiomers. Therefore, chiral analysis and chirality are paramount in chemical, biological, and pharmaceutical technologies and modern chemistry. However, because enantiomers have the same chemical and physical characteristics in an achiral environment, chiral separation has long been believed to be one of the most complicated analytical separations. Nevertheless, numerous improved techniques have been developed by creating an exceptional chiral climate using various chiral solid substances. Subsequently, analytical methods play an indispensable role in differentiating enantiomers as more scientists become aware of the significance of chirality [2].

2. Principles of Chiral Analysis

Chiral studies refer to stereoisomer separation. Two enantiomers have the same physicochemical characteristics, such as molecular weight and substituent groups. The enantiomers lead to the rotation of polarized light in the reverse direction with diversely substituent groups orientated in a 3D space. However, these groups are oriented diversely in the area. According to this feature, they lead to polarized light rotation in the opposite direction. Therefore, for the separation of chiral analytes, creating or selecting a suitable chiral environment is of paramount importance due to the potential of enantiomers having a stereo-specific interaction with that chiral environment [8].

The enantiomers can be separated by applying two approaches: indirect and direct resolution. In an indirect resolution, a chiral compound reacts with the chiral derivatization agent and produces stable diastereomeric complexes; chemical bonds are formed. Generally, chiral derivatization requires easily derivatizable functional groups, such as carboxylic acids, amines, thiols, and hydroxyls, in the analyte that is in contiguity with the stereogenic center [2]. In a direct approach, enantiomers interact with a chiral selector (CS), which leads to the production of labile diastereomeric compounds with weak bonds included. The environment of the separation system contains the chiral selector. [9].

From a mechanistic point of view, chiral identification is commonly assumed to necessitate a three-point interaction arising from the stereogenic centers of the chiral analyte and selector. Therefore, generating transient diastereomers as exploits of chiral separations usually needs a primary docking mechanism between the chiral analyte and the CS, together with a mixture of secondary interactions describing the stereo-specificity of the interaction [10]. These mechanisms contain a π -acid: π -base, an electrostatic or an inclusion complexation. However, suchlike instruments often rely on the primary interaction between the chiral chemical and the CS in a given experimental setting. However, the secondary interactions involve hydrogen bonding steric, dispersion, or dipole-dipole interactions, so they are commonly weaker than the primary docking mechanism [2]. Most of the chiral selectors provide various possible interaction sites. Chiral compounds may have non-stereo-specific interactions with the chiral moiety of the CS if the relative orientations of their stereogenic aspects prevent stereo-specific interactions. Non-stereo-specific interactions between the CS and the chiral compounds are usually parasitical to the enantioseparation [2]. It is worth noting that alterations in the experimental conditions can cause changes in the primary docking mechanism. For instance, alterations in pH that change the ionization of different functionalities within the CS or the chiral compound affect the primary docking mechanism, thereby converting enantiomer separation [11].

In selecting the most well-suited methods for the discrimination of enantiomers, the first step is to consider which analytes' properties should be separated, such as their solubility and volatility. Numerous analytical methods have been developed for chirality determination and separation throughout the last many decades. These approaches include high-performance liquid chromatography (HPLC) [12], capillary electrophoresis [13], capillary electrochromatography (CEC) [14], fluorescence spectrometry [15], gas chromatography (GC) [16], supercritical fluid chromatography [17], high-speed countercurrent chromatography [18], chemiluminescence [19], nuclear magnetic resonance spectroscopy [20],

mass spectrometry [21], immunoassays [22], and electrochemistry [23]. This article reviews chiral recognition techniques, such as sensors, HPLC, GC, and CEC, to analyze biologically active compounds (e.g., racemic drugs, amino acids, and biological molecules) using so-called functional materials.

3. The Attraction of Functional Materials in Chirality

In the 21st century, materials science is one of the most attractive search fields in natural sciences. A survey of the literature from the past years clearly shows that the application of functional materials in chiral recognition techniques has also become the center of researchers' attention. A variety of functional materials involving nanoparticles (NPs), MOFs, molecularly imprinted polymers, ionic liquids (ILs), covalent organic frameworks (COFs), deep-eutectic solvents (DESs), porous organic cages (POCs), and some other porous organic materials (like metal–organic cages), have been successfully employed in chiral sensors, CE, and HPLC [24–27]. There are two driving forces behind this: one is the continuous progress of functional materials and the steady stream of novel capabilities that are being recognized, and the second is the innate flexibility of the mentioned strategies (sensors, CE, and HPLC) that guarantees the use of these materials.

Theoretically, there is an infinite variety of advanced materials for screening and evaluating. More significantly, researchers can adjust the enantio-separation ability of these functional materials by managing their morphologies or structures. Thus, the growth of new chiral selectors is based more on a “design-driven” approach than the “screening-based” method, which is much more appealing and proficient [24]. Moreover, to be used as CSPs/CSs, these advanced materials can also act as additional additives for modification of the electroosmotic flow or to enhance peak shapes (such as NPs, DESs, ILs), as background electrolytes (like ILs), or as support/coating/packing materials for improving the mass transfer and phase ratio during separations (for instance COFs, MOFs, NPs) [26,28,29]. According to these attributes, the potential of advanced materials in chiral analysis seems boundless. Therefore, this article offers an overview of the state-of-art MOFs in chiral science, focusing on sensors, CEC, and chromatographic technologies. The authors will focus on inventive concepts and highlight important topics in this field, especially in the preceding decade.

4. Metal–Organic Frameworks in Chiral Analysis

MOFs, also called porous coordination polymers, are a novel category of microporous crystalline materials employed in chiral separation. MOFs are one-dimensional (1D), two-dimensional (2D), or 3D inorganic–organic porous hybrid materials assembled from rigid metal clusters or metal ions (nodes) and flexible organic linkers (such as phosphonates or carboxylates) [30]. They provide unique chemical characteristics with substantial and permanent inner porosity. Additionally, MOF structures have exceptional diversity due to their functionalization and framework architecture [31]. Due to their numerous novel properties, including having a large surface area, excellent thermal and chemical stability, high porosity, non-toxic nature, and available cavities and tunnels, MOFs are attractive substances for chiral separation. Their ultra-high surface areas of up to $10,000 \text{ m}^2 \text{ g}^{-1}$ are one of the main factors making them superior to other porous materials [32]. MOFs' structural differences, crystalline nature, and structural details make them an appropriate candidate in various areas, such as chemical sensing, separation, drug carrying, biomedicine, proton conduction process, and catalysis, in the last two decades [33].

Combining MOFs' porosity with chirality offers platforms that initiate the design of chiral MOFs (CMOFs) or chiral porous coordination polymers. These types of MOF-based chiral compounds can be created with numerous constituents that can form distinct frameworks with different usages, such as enantiomer separation and asymmetric catalysis [34]. CMOFs are a more significant part of chiral inorganic-organic hybrid compounds and a subset of MOFs possessing extreme enantiomer separation functions. CMOFs have attracted considerable scientific attention, especially in the last decade, for two chief reasons: first,

the significance of the structure, either in topology or architecture; and second, their applications in a broad spectrum of fields, such as enantioseparation, chiral sensing, asymmetric catalysis, and ferroelectric area (Figure 1) [35]. Furthermore, there are other recent advances in the use of CMOFs in a variety of topics, such as second-order nonlinear optics (NLO), circularly polarized luminescence (CPL), photoelectrochemical sensing, drug delivery (DD), green analytical chemistry (GAC), such as analytical sample preparation (as unique sorbents) and microextraction (micro-solid-phase extraction (μ -SPE)) techniques [36,37].

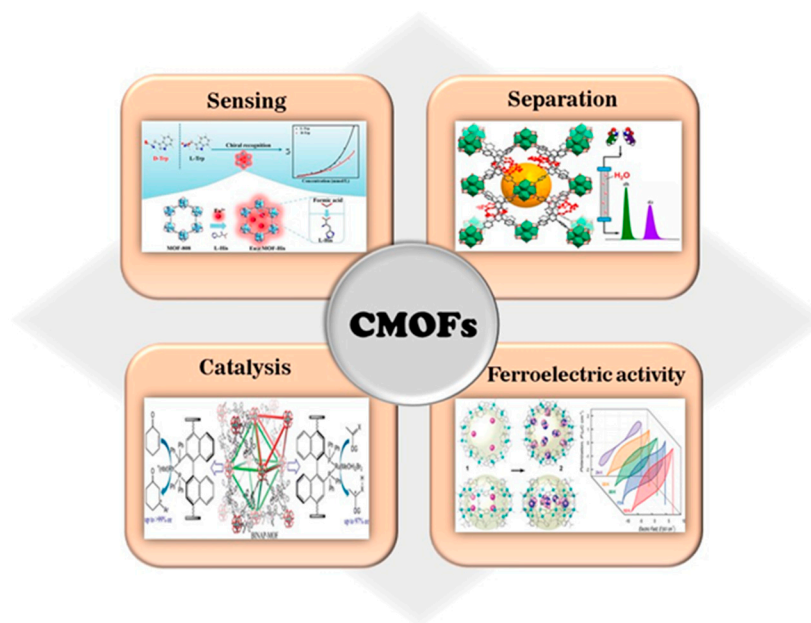
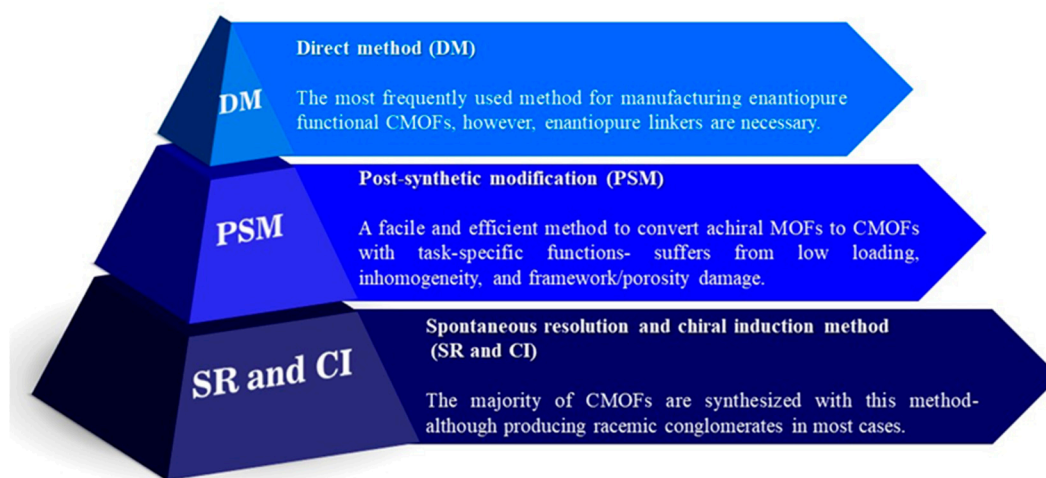


Figure 1. Category of chiral MOFs applications.

In principle, chirality in CMOFs can emerge because of chiral agents in an asymmetric environment, precursors (sometimes both) and through specific alignments of achiral precursors that result in instinctive discrimination [38]. CMOFs can be synthesized through three strategies (Figure 2): (I) The spontaneous resolution and chiral induction method (SR and CI), the formation of chirality over spontaneous resolution, or crystal growth that can be referred to as the physical arrangement and nature of precursors. It indicates that the spatial placement of an achiral building block via enantiospecific supramolecular interaction causes crystallizing MOFs in a chiral set. (II) The indirect method is the post-synthetic modification (PSM) method in which achiral frameworks are formed, and external chiral agents (chiral guest, temperature, solvent, and auxiliary pendant) are employed to produce stereogenic centers. (III) The most significant, effective, and reliable methods for generating CMOFs include applying a chiral node (either metal cluster or ion), linker, or combination. This process is the last technique and is named the direct method (DM) of chiralization. Research has confirmed that this method results in CMOFs with novel characteristics [39]. It is worth noting that crystallographic measurements are accurate and crucial proofs for the confirmation of the chirality generated in the structure. Hence, the metal's electronic/geometric configuration at the node position of metal–organic frameworks might alter their characteristics with asymmetric orientation formed throughout crystallization, which is a crucial agent in creating SR-derived CMOFs [40].

Furthermore, CMOFs can be categorized into two major classes based on chirality type: heterochiral and homochiral. The outcome of chiral organic moieties with the same handedness can be homochirality, which additionally possesses optical centers; they can have conformational rigidity and considerable length [41]. However, in heterochirality, ligands with opposite handedness create a heterochiral complex configuration [42]. Although the fabrication of homochiral configurations is preferable in the literature, sometimes het-

erochirality leads to novel and practical attributes that homochirality does not display. In this compound, heterochiral interactions serve an efficient role in the construction of crystalline racemates. In racemate configurations, heterochiral interactions demonstrate the capability of overcoming homochiral interactions [41]. The main factor that makes chiral materials so popular is their extremely fascinating potential applications. According to the characteristic attributes of MOFs alongside their chirality performance, CMOFs provide extraordinary opportunities for novel applications. However, employing CMOFs and focusing on their specific properties have been under discussion in the past. Nevertheless, it is a real challenge for researchers to obtain CMOFs with the lowest cost and highest performance. Fabrication techniques, pore size, type, and functionality, in addition to the MOF nature, are significant parameters affecting the choice of application [43].



Synthetic Methods of CMOFs

Figure 2. Three synthetic methods of chiral MOFs with a summary of their merits and drawbacks.

Regarding the significance of chiral recognition of active compounds, as described in the previous sections, in the production of pharmaceuticals, especially biological processes, determining one enantiomer from the racemic composite is paramount in chirotechnology. More precisely, enantiomers with identical chemical and physical characteristics present researchers with a significant challenge. To overcome this problem, chiral recognition and separation methods require efficient compounds with the separating capability of enantiomers in addition to great enantioselectivity. At first, chiral zeolites were used for this purpose. Still, since the merits (such as high surface area, diverseness in pore size and structure, selective adsorption affinity, and special microporosity) of MOFs/CMOFs were higher than zeolites, researchers have become enthusiastic about employing them [44,45]. The chiral discrimination and separation are related to the two enantiomers' differing orientations and binding energies inside the MOF's microenvironment. However, the orientation and potential map of the (S)-enantiomer differ significantly from those of the (R)-enantiomer, and the specific binding energies differ. Consequently, enantioselective adsorption is predicted due to changes in binding energy and orientation [46]. Based on the literature in the past few years, MOFs can be used as the perfect candidates for the enantioseparation of different compounds [47]. Thus, chiral recognition and separation using CMOFs are within the scope of this review. This property of CMOFs refers to their ability to interact with guest molecules, such as ion exchange; electrostatic mechanism forming inclusion complexes; hydrogen bonding; dipole-dipole, steric, and hydrophobic interactions. Herein, we discussed the application of CMOFs for chiral recognition and the separation of racemate compounds using sensors, chromatographic techniques, and CEC.

5. Metal–Organic Frameworks for Designing Enantioselective Sensors

This section reviews the application of CMOFs for the chiral recognition of racemate compounds using different types of sensors. Generally, the chiral sensing phenomenon depends on two primary processes: signal transduction and molecular recognition. Designing molecular structures providing sites for enantioselective recognition with various interaction affinity for enantiomers of racemic materials is the fundamental factor in fabricating reliable chiral (bio)sensors [48]. It is essential to have a chiral surface or environment for differentiating the enantiomers. In the sensors, possessing the signal of enantioselective identification requires specific interactions of enantiomers with a chiral selector. Therein, it is worth noting that the “lock-key” rule and phenomenon of the “three points interactions” are facilitated methods suggested so far for the enantioselective interaction scenario. Hence, chirality-based (bio)sensors generally relate to host-guest chemistry via non-covalent interactions, such as π - π interactions and hydrogen bonding. Numerous driving forces reinforce the interactions between guest and host molecules, leading to enantioselective identification. To develop selective and efficient enantiomer recognition, the host’s structure needs to create several driving forces with guest molecules [49].

Recently, a variety of strategies have been employed for developing chiral sensors. Herein, MOFs have emerged as an exciting material because of their porosity, high surface area, and capability of adsorbing guest molecules to design susceptible platforms named chirality-based sensors [49]. In general, MOFs possess different chemical and physical features and topological structures. CMOFs show enormous potential in the chiral identification field [50]. MOFs’ porous structure can preconcentrate the target to obtain improved sensitivity. Meanwhile, the channels and pores can render an ideal medium for accommodating the target molecules, which provokes special recognition. The selectivity of sensors developed based on MOFs is derived from (i) the chirality of the framework, (ii) channel size exclusion, (iii) host-guest chemistry in the MOF cavity, (iv) target-specific signal response, and (v) hydrogen bonding or specific coordination of analytes to the framework [51]. Principally, any alterations in the properties of MOFs based on the type of guest molecule should be evaluated as a sensing signal. The sensitivity of MOF detection mainly relates to the sensing technique employed for signal transduction [31].

In this section, we will summarize developed CMOF-based enantioselective (bio)sensors and discuss the fundamentals of their performances. For the sake of specificity, this section is in parts: fluorescence, electrochemical, quartz crystal microbalance (QCM), and circular dichroism (CD) (bio)sensors based on thermal transduction.

5.1. Fluorescence Enantioselective (Bio)Sensor

Fluorescence (bio)sensors are label-based optical (bio)sensors that have been offered as an alternative to the electrochemical approaches discussed below. These (bio)sensors utilize quantum dots (QDs), fluorescence proteins, and dyes as labels. Some characteristics, such as the real-time and direct detection of various chemical and biological materials, provide them a distinct edge over traditional analytical procedures [52,53]. Fluorescence offers several signaling modes for detecting substrate than electronic absorption, including fluorescence amplification, quenching, exciplexes, excimers, and lifetimes. The sensitivity of fluorescence methods needs relatively small amounts of sensor molecules. Recently, there has also been an increase in interest in developing fluorescence sensors for the enantioselective detection of chiral compounds. These sensors have the potential to provide a real-time approach for the recognition of the enantiomeric composition of racemic compounds, which might considerably allow quick analysis of chiral molecules [54,55]. Chiral biphenyl or binaphthyl composites are popular fluorophores commonly applied as optical (bio)sensors for enantiomer recognition because of their innate particularities, such as rigid enantiomeric conformation, excellent emission efficiency, C2 axial chirality, and easily selective functionalization [37]. In 2012, Lin et al. hypothesized that an outstanding procedure for enantioselective sensing could be supplied by making use of CMOFs as well as the internment effect of the framework and rigid configuration of sens-

ing moieties for increasing stereoselectivity [56]. A secondary building unit, a cadmium carboxylate infinite-chain, and 1,1'-bi-2-naphthol-derived chiral tetracarboxylate bridging ligand was used for the construction of a fluorescent and highly porous MOF (Figure 3). Amino alcohols led to the efficient quenching of the fluorescence of the fabricated MOF through hydrogen binding with the binaphthol moieties decorating it. This resulted in the fabrication of a binaphthol-based homogeneous platform as a remarkable enantiomer recognition sensor for amino alcohols with highly improved enantioselectivity and sensitivity. The R and S enantiomers various amino alcohols, including 2-amino-1-propanol, 2-amino-2-phenylethanol, 2-amino-3-phenylpropanol, and 2-amino-3-methyl-1-butanol, underwent enantioselective recognition by the MOF-based chiral fluorescence sensor. Various amounts of amino alcohol quenchers were used to measure the fluorescence signals of the MOF suspensions. The created MOF was a very sensitive fluorescent sensor with excellent fluorescence quenching thanks to the four chiral amino alcohols. This was followed by Stern-Volmer (SV) behavior, which provides precious information in the clarification of the photocatalytic reaction mechanism in the concentration range of 0–4 μM with remarkably high KSV (SV constants) of 490–31,200 M^{-1} due to analyte absorption and preconcentration inside the cavities of the MOF. At the same time, its higher enantioselectivity is assumed to be a result of increased enantiomer discrimination related to the confinement effect of the cavity and the rigid configuration of the binaphthol moieties in the framework.

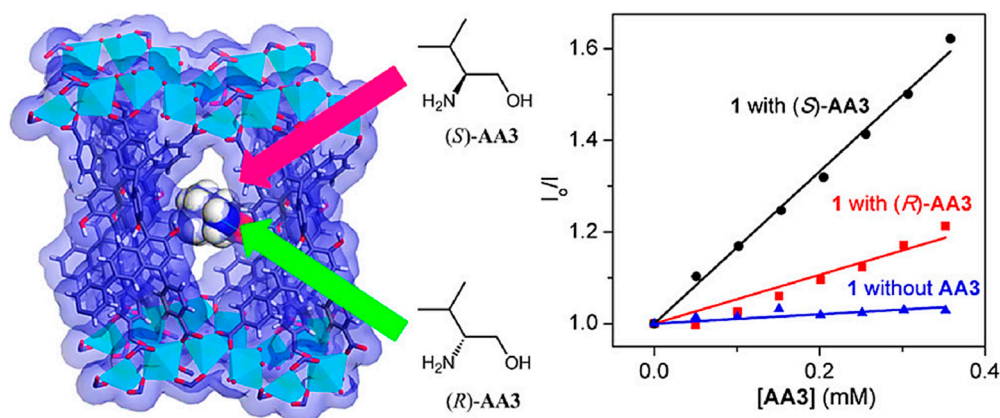


Figure 3. An illustration of analyte inside a synthesized fluorescent and highly porous MOF channel and amino alcohol quenchers' chemical structures. As well as the Stern-Volmer plot for quencher 2-amino-3-phenylpropanol (AA3) added to CMOF. Reprinted (adapted) with permission from [56]. Copyright 2012 American Chemical Society.

Approximately four years later, Moorthy and colleagues designed a water-stable and incredibly luminescent homochiral anionic CMOF termed Zn-MOF. For instance, Zn-PLA was based on the metal-assisted self-assembly of a fluorescent chiral pyrene-tetralactic acid (H_4PLA), which naturally inspects concave structures for guest inclusion, with $\text{Zn}(\text{NO}_3)_2$ to investigate the chiral sensing of amino acids through fluorescence quenching [57]. Treatment of the organic linker H_4PLA with $\text{Zn}(\text{NO}_3)_2$ resulted in the creation of luminescent and porous crystals of Zn-PLA. Among all amino acids, such as cysteine (Cys), histidine (His), tryptophan (Trp), and tyrosine (Tyr), His led to the selective fluorescence quenching of Zn-PLA aqueous dispersion due to the exchange of the cationic species of dimethylammonium (DMA) in the MOF crystals through His, which is protonated in water. DMA was stabilized inside the voids through robust hydrogen binding with the carboxyl groups of PLA. The cationic imidazolium ring of His is believed to contribute to charge-transfer interactions with the excited state of protected pyrene fluorophore for observing quenching. The selective sensing of His is of paramount importance because of its relation to different biological functions. The chirality of MOF, which is related to lactic acid groups, resulted in

the enantioselective sensing of the D and L enantiomers of His with an enantioselectivity ratio of 1.8 from the SV quenching plots.

For the first time, in 2018, for the fluorescent enantioselective sensing of chiral α -ethylbenzylamine, Bu and colleagues generated a whole new class of stereoisomeric porous homochiral MOFs, including isorecticular, diastereomeric, and enantiomeric MOFs, with various metal nodes in the absence or presence of a secondary linker [58]. Isocamphorate generates unpredictable framework topologies from regular inorganic building blocks, and isocamphoric acid enables the achievement of numerous novel homochiral compounds. Generally, the 3D CMOF constructed of copper dimers and RR-cam supported by 4,4'-bipyridine ligands, named CPM-332-RR or $[\text{Cu}_2(\text{RR-cam})_2(\text{bpy})]$, exhibited enantioselective fluorescent quenching for α -ethylbenzylamine enantiomers. Moreover, these easily accessible chiral ligands, created from converting previously existing chiral ligands, will pave the way for incrementing MOF-based enantioselective platforms. Recently, Shi and colleagues reported the integration of chirality and luminescence in MOFs for improving luminescent sensors [59]. For this purpose, five chiral sites containing N-benzylquininium chloride were introduced into an anionic luminescent Zn-based MOF through a simple cation exchange method. A CMOF was fabricated with dual luminescent centers composed of the Tb^{3+} ions and ligand (Zn-MOF-C-Tb). Significantly, the designed luminescent and chiral bifunctional dual luminescent centered-MOF exhibited the enantioselective identification of amino alcohol enantiomers and cinchonidine and cinchonine epimers. In all cases, the developed Zn-MOF-C-Tb demonstrated wonderful enantioselectivity. The N-benzylcinchoninium chloride, S-2-amino-1-propanol, and S-2-amino-1-butanol had faster fluorescence quenching than their related enantiomers, indicating the broader usage of the suggested bifunctional MOF platform. The relative standard deviation (RSD) for the I544/I354 (intensity 544 nm/intensity 354) ratio was considerably lower than that of employing just the I544 emission. This showed the benefit of reduced system errors in the ratiometric sensing platform. The quenching capability of Zn-MOF-C-Tb was evaluated by recycling experiments and stability tests in the presence of cinchonidine and cinchonine with 6 cycles at 544 nm. The ratio of quenching was between 97.1% and 98.1%. The bifunctional Zn-MOF-C-Tb showed a method for the enantioselective recognition of chiral molecules with reusability and excellent stability.

In 2022, Yan et al. developed a CMOF-His through post-synthetic ligand exchange using L-His as a chiral center and its immobilization into a zirconium (Zr)-based MOF [60]. For this purpose, water-stable and modifiable MOF-808 as a Zr(IV)-based MOF with high inherent peroxidase-like catalytic activity under alkaline, neutral, and acidic conditions was employed as the parent skeleton, and L-His was partially replaced with the formic acid ligand. Then Eu^{3+} ions were introduced as a new luminescence center by hybridizing then with MOF-His to have the final composite Eu@MOF-His (Figure 4). The bifunctional Eu@MOF-His had both enantioselective luminescence and chiral characteristics among many amino acids. By decreasing the enantiomer concentration to the range of 0–0.35 mM, there was a good linear relationship between the fluorescence intensity of the prepared MOF in the water (I_0)/substrate solution (I) at 614 nm (I_0/I) and the substrate concentration. The quenching constants KSV of D-Trp and L-Trp were 12,547 and 19,154 M^{-1} , respectively. The quenching constants ratio of L-Trp/D-Trp was 1.53, indicating that the two enantiomers had discrepant quenching rates. The detection limit of Eu@MOF-His for D-Trp and L-Trp was 4.1 and 2.7 μM , respectively. Therefore, Eu@MOF-His was appropriate for the Trp enantiomers detection in a low concentration. Based on the obtained results, enantiomers of Trp can efficiently quench the Eu^{3+} ion's red-light emission. Moreover, the quenching rates were different, stemming from the diversity of the analytes' interactions with the chiral recognition sites. Eu@MOF-His restored its fluorescence intensity to 614 nm after 4 cycles, demonstrating that the prepared MOF can be used to detect Trp enantiomers. The designed Eu@MOF-His displayed the potential of being a tremendous fluorescent sensor for recognizing Trp enantiomers due to its high sensitivity, rapid response, and reusability.

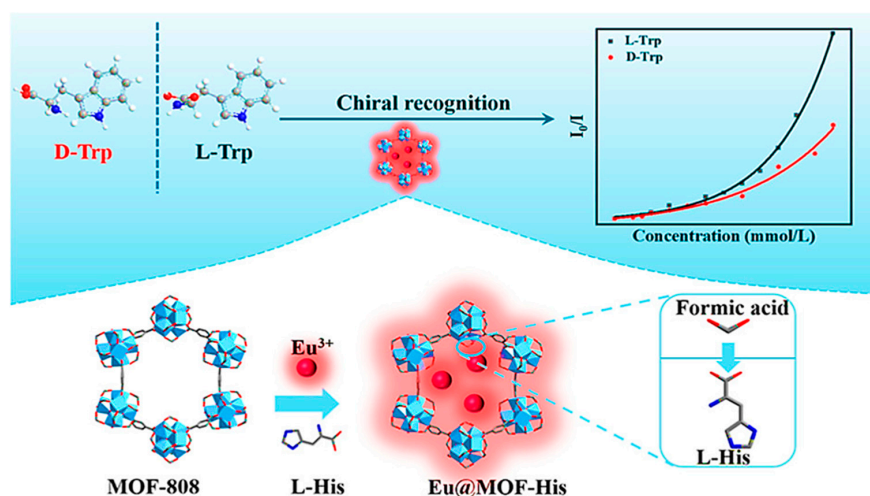


Figure 4. Preparation steps and application of Eu@MOF-His for fluorescence enantioselective sensing of tryptophan. Reprinted (adapted) with permission from [60]. Copyright 2022 American Chemical Society.

In 2022, Zhu et al. synthesized poly (amidoamine) (PAMAM) dendrimers-functionalized achiral luminescent MOF, termed MIL-53(Al)-NH₂, for the fast enantioselective sensing of lysine (Lys). MIL-53(Al)-NH₂ was an Al-based MOF that was synthesized with 2-aminoterephthalic acid and AlCl₃ (Figure 5) [61]. Then, the modification of the synthesized MOF with PAMAM, called PLMOF, led to the enhancement of fluorescence intensity, and by the dispersion of PAMAM-modified MIL-53(Al)-NH₂ to water, the achieved solution showed excellent stability and fluorescence intensity. The fluorescence of the luminescent MOF solution was quenched for amino acid detection by adding the Cu²⁺ concentration. Adding the Lys enantiomers to the PLMOF solution caused the partial restoration of the quenched fluorescence signal due to the powerful chelation between Cu²⁺ and Lys. In such circumstances, the fluorescent signal of the unique fluorescence MIL-53(Al)-NH₂-PAMAM-Cu²⁺ sensor entered “turn-on” mode due to the various chelation potentials, which led to the sensitive enantioselective determination of D-Lys and L-Lys by fluorescence intensities. The results exhibited successful enantioselective detection of D/L-Lys with good linearity and detection limits of 12.2 and 7.52 μM for D-Lys and L-Lys, respectively. The PAMAM-grafted luminescent MOFs demonstrated good fluorescence intensity stability under prolonged UV irradiation. The RSDs of interday and intraday fluorescence intensities were 1.01% and 1.07%, respectively, expressing the excellent repeatability and stability of PAMAM-grafted luminescent MOFs in the detection process.

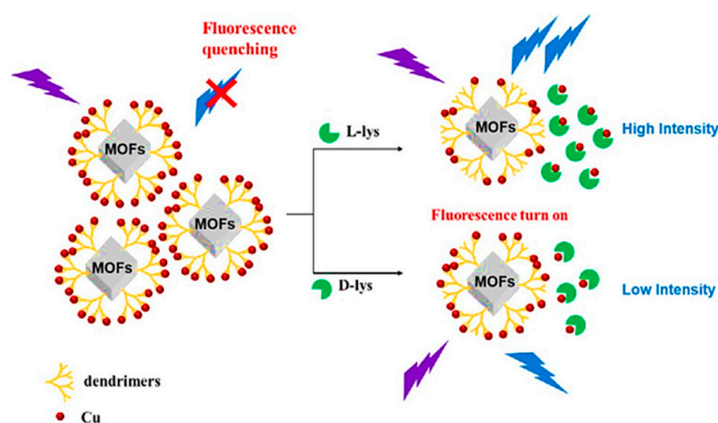


Figure 5. Achiral luminescent MOFs grafted onto PAMAM for enantioselective sensing of lysine enantiomers. Reprinted (adapted) with permission from [61].

5.2. Circular Dichroism Enantioselective (Bio)Sensor

CD spectroscopy is one of the robust techniques in stereochemical analysis and is usually for molecular recognition and absolute configuration assignment [62]. It is among the existing approaches for enantioselective recognition, such as capillary electrophoresis, chromatography, and fluorescence. Conventional CE and chromatography techniques are efficient for the racemic resolution of a broad spectrum of chiral analytes. However, these systems have several limitations, including complex programming, high cost, and time consumption, which hinder convenience and quick and easy enantioselective recognition. Although fluorescence (bio)sensors can recognize the enantiomers effectively and quickly, the downside of this approach is that the only suitable candidates for this type of (bio)sensor are vigorous luminescent materials. In addition, the visual reflection of stereochemical signs related to detected chiral molecules cannot be obtained from fluorescence (bio)sensors [63]. CD is the most frequently employed technique for visual chirality with a broad spectrum of applications in exploring charge-transfer transitions [64], the secondary structure of proteins [65], and the electronic and geometric structure of compounds [66]. Fluorescence exhibits attributes such as rapidity and the molecular absolute configuration of probed chiral substances [66]. In general, the sensing procedure of CD-(bio)sensors is achieved by forming a coordinative or covalent bond via pesky chemical reactions between originally UV-active and CD-silent molecules. This can result in an asymmetric induction to generate a favored chiral structure population with different chiroptical yields. Therefore, it is significant to advance an appropriate and faster technique to obtain effective sensing in which weak supramolecular interactions are introduced into the inclusion composites. On this matter, CMOFs with numerous chiral recognition sites and a limited effect are great candidates for CD sensors [67].

The first application of a CMOF for an enantioselective CD-(bio)sensor was reported by Zhang and colleagues in 2015 [67]. A pair of homochiral zeolitic imidazolate-related frameworks (HZIRFs) with sodalite topology, including (R)-2-(1-hydroxyethyl) benzimidazole [(R)-OH-bim] and (S)-2-(1-hydroxyethyl) benzimidazole [(S)-OH-bim], was achieved by both chiral benzimidazole and tetrazole ligands. The successful accomplishment of bulky zeotype and homochirality configurations in HZIRFs was influenced by the assistance of another ligand, 5-methyltetrazole, and adding a chiral C center into the benzimidazole ligand. The homochiral zeolitic imidazolate-related framework topological configuration with abundant H-bonding medium in the ethanol solutions of chiral carvone exhibited CD-sensitivity. By adding the HZIRFs-R, the CD signals remarkably decreased for both L- and D-carvone. Nonetheless, L-carvone showed a significant signal decrease compared to D-carvone, proposing a strong interaction between L-carvone and the CMOF. Based on the obtained results, the chiral recognition happened on the external surface of HZIRFs-R because its small window size blocks the entry of carvone. The same research team expanded this procedure for synthesizing a series of more microporous homochiral zeolitic CMOFs (ZMOFs) [68]. They synthesized four types of homochiral ZMOFs by mixing 5-methyltetrazole ligand and various amino acids, including L-alanine, D-alanine, L-serine, and L-valine, as linkers named $Zn_4(5\text{-mtz})_6(\text{L-Ala})_{2.2}(\text{DMF})$, $Zn_4(5\text{-mtz})_6(\text{D-Ala})_{2.2}(\text{DMF})$, $Zn_4(5\text{-mtz})_6(\text{L-Ser})_{2.2}(\text{DMF})$, and $Zn_4(5\text{-mtz})_6(\text{L-Val})_{2.2}(\text{DMF})$ for the chiral sensing of the carvone. For the chiral determination of the carvone, the CD signal of a solution of L-carvone or D-carvone and four as-synthesized samples was recorded. The result indicated that D-carvone and L-amino acid-based samples had stronger interactions than the interactions of L-carvone and L-amino acid-based samples. At the same time, L-carvone had stronger interactions with $Zn_4(5\text{-mtz})_6(\text{D-Ala})_{2.2}(\text{DMF})$. The separation enantiomeric excess (ee) values of L-amino acid-based samples, including $Zn_4(5\text{-mtz})_6(\text{L-Ser})_{2.2}(\text{DMF})$, $Zn_4(5\text{-mtz})_6(\text{L-Ala})_{2.2}(\text{DMF})$, and $Zn_4(5\text{-mtz})_6(\text{L-Val})_{2.2}(\text{DMF})$, were 43.2%, 18.6%, and 25.8%, respectively. $Zn_4(5\text{-mtz})_6(\text{L-Ser})_{2.2}(\text{DMF})$ had the most significant separation capability due to the $-\text{OH}$ groups improving the $Zn_4(5\text{-mtz})_6(\text{L-Ser})_{2.2}(\text{DMF})$ interaction with the carvone.

Two years later, Zhang et al. presented a systematic study of CMOF-based CD sensors for eight pairs of L/D-amino acids [69]. Self-assembly of (1R,2R)-2-(pyridine-4-ylcarbamoyl) cyclohexanecarboxylic acid (RR-PCCHC), a rationally created chiral ligand, with $Zn(NO_3)_2$ resulting in the fabrication of a 2D water-stable homochiral MOF [$Zn(RR-PCCHC)_2$] (HMOF-1), which is composed of a DNA-like right-handed double-helix structure. The synthesized HMOF-1 demonstrated great thermal and solvent stability, as well as stability in weak basic, weak acidic, and neutral aqueous solutions. Moreover, emulsified HMOF-1 exhibited a strong innate CD signal in an aqueous solution. Adding various amino acids decreased the strength of HMOF-1's CD signals. Notably, the emulsified HMOF-1 determined aspartic acid (Asp) with a limit of detection (LOD) of 13.31 ppm and 92.1% recognition efficiency for L-Asp (Figure 6). By doing titration studies using α -hydroxyl carboxylic acids, D/L-lactic acid, and (R,R)/(S,S)-tartaric acid, the universality of the proposed CD-sensor application was tested. By adding various volumes of α -hydroxyl carboxylic acids, emulsified HMOF-1 showed a similar CD signal intensity alteration. The CD signal intensity of emulsified HMOF-1 significantly decreased as a result of (R,R)/(S,S)-tartaric acid, with (S,S)-tartaric acid having a more significant impact than (R,R)-tartaric acid. At the same time, D/L-lactic acid resulted in a minimal effect on the CD signal's intensity. Recognition efficiency (η) of (R,R)-tartaric acid was 37.5%, while that of (S,S)-tartaric acid was 53.2%. The obtained results showed the ability of HMOF-1 in the sensitive recognition of enantiomeric carboxylic acids. DNA-like HMOF-1 demonstrated an interaction mechanism with probed amino acids like the groove binding of DNA with a targeting drug.

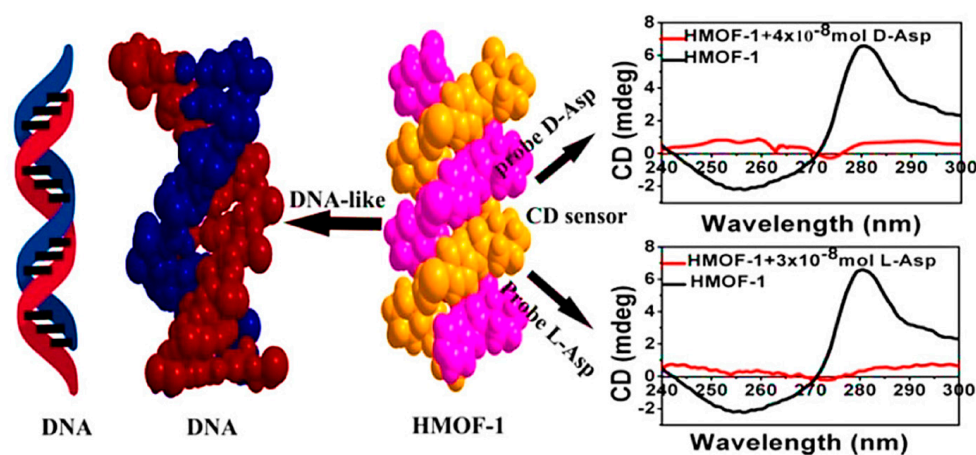


Figure 6. Schematic illustration of the CD spectra of D/L-aspartic acid and a space-filling image of the right-handed double helix HMOF-1. Reprinted (adapted) with permission from [69]. Copyright 2017 American Chemical Society.

After a short time, the same research group focused on the preparation of three new chiral 3D metal-carboxylate frameworks termed $[M_2(bptc)(H_2O)(MeOH)] \cdot 3H_2O$ ($M = Ni, Co, CoNi$, $bptc^{4-} = 3,3',5,5'$ -biphenyltetracarboxylate), which spotlight chiral 4-fold helical metal chains, such as SBUs (secondary building units), for enantioselective CD-sensors [70]. The reaction of biphenyl-3,3,5,5-tetracarboxylic acid as an achiral ligand with Ni^{2+} , Co^{2+} and their mixture created three stable, isostructural porous chirality-enriched MOFs: Ni-MOF, Co-MOF, and CoNi-MOF. Specifically, Co-MOF exhibited sensitive and fast CD sensing of a variety of racemic α -hydroxy/amino acids, and 38.59% was the largest relative difference in the CD signals of L/D-mandelic acid. In 2021, Jiao and co-workers developed an enantioselective CD sensor by designing a homochiral MOF named $[Zn(L)(2,2'-bipy)] \cdot H_2O$ (LNNU-1) in which ($H_2L = HOOC-C_6H_4-CH_2PO(OH)(OC_2H_5)$) and 2,2'-bipy = 2,2'-bipyridine were used as two organic ligands with aromatic ring and carboxy phosphonic groups. LNNU-1 had several noncovalent interactions with Trp [71]. They did not observe any induced circular dichroism (ICD) signals for all-natural amino acids, DL-Trp, and D-Trp pure aqueous solutions, as well as aqueous solutions of LNNU-1 without enantiomers of Trp. However,

adding LNU-1 to the mixture of Trp enantiomers and all other natural amino acids aqueous solution led to the observation of a strong ICD signal. Blood plasma was used to test LNU-1's selectivity for common compounds that did not exhibit an ICD signal, except signals of the enantiomers of Trp. Numerous noncovalent interactions between chiral Trp and LNU-1 led to the emergence of an intense, induced CD signal. This resulted in the precise detection of the absolute configuration and enantiomeric ratio of nonracemic Trp specimens in blood plasma constituents and the mixture of natural amino acids' aqueous solution. Moreover, the enantioselectivity mechanism of the sensor was also examined. It is worth noting that the designed CD sensor resolves the problems related to traditional determination techniques for amino acids, including non-repeatability, high cost, complex operation, and time-consumption. The developed system showed high selectivity and reliability for enantiomers sensing through homochiral MOF-ICD sensors.

5.3. Quartz Crystal Microbalance Enantioselective (Bio)Sensor

The QCM is a portable and ultrasensitive device for chemical sensors with the potential to sense mass alterations in the range of nanograms. It has been pleasantly employed for various applications, especially the selective sensing of enantiomers. The chiral recognition layer on the surface of quartz is one of the cardinal parameters for obtaining high specificity and sensitivity. Various chiral substances, such as synthetic macromolecules, molecular imprinting polymers, amino acids, and proteins, have been widely used to fabricate chiral QCM sensors. CMOFs with tunable and abundant recognition sites are for such functions [72,73]. The proliferation of a thin film of CMOFs on a quartz surface is named surface-mounted MOFs (SURMOFs), which empower the development of CMOF-based QCM sensors [74].

In 2012, an early report on integrating a QCM-sensor and a CMOF was conducted by Fischer and Wöll et al. [73]. The layer-by-layer liquid-phase epitaxial (LPE) growth technique was applied for the growth of enantiopure SURMOF coatings of $[\{Zn_2((-)cam)_2(dabco)\}_n]$ and $[\{Zn_2(+)cam)_2(dabco)\}_n]$ through dipping the QCM substrate with a dabco linker, equimolar chiral camphoric acid, and $Zn(Ac)_2$. The thin film of an enantiopure surface-mounted MOF $[\{Zn_2((\pm)cam)_2(dabco)\}_n]$ on the surface of the QCM enabled the enantioadsorption of the selected enantiomeric probe molecules S-HDO ((2S,5S)-2,5-hexanediol) and R-HDO ((2R,5R)-2,5-hexanediol) from the vapor phase in a continuous flow mode using nitrogen gas as a carrier. Based on the achieved results, $[\{Zn_2(+)cam)_2(dabco)\}_n]$ had almost 1.5-fold higher adsorption for R-HDO than S-HDO. Dissimilarity in the rate of absolute uptake and absorption for the chosen enantiomeric target molecules resulted in the discovered enantioselectivity. Extending this procedure by Gu and Xu et al. in 2019, thin films of $[Zn_2Cam_2DAP]_n$, an azapyrene-based CMOF, were grown on the functionalized substrate for the development of a QCM-sensor, which was termed SURchirMOF $[Zn_2Cam_2DAP]_n$ [75]. The designed SURchirMOF $[Zn_2Cam_2DAP]_n$ was based on chiral camphoric acid layers and 2,7-diazapyrene ligands through an LPE layer-by-layer technique similar to the structure of $[\{Zn_2(+)cam)_2(dabco)\}_n]$. D/L-methyl-lactate enantiomers were used for evaluation. D-SURchirMOF-4 had the adsorption amount of ~ 3.54 (ML) and ~ 2.08 (MD) $\mu g/cm^2$ for L- and D-methyl-lactate, respectively. Additionally, D/L-methyl-lactate enantiomers were employed for investigating the L-SURchirMOF-4 enantioselective adsorption, which showed ~ 2.02 (ML) and ~ 3.62 (MD) $\mu g/cm^2$, the adsorption amounts for L- and D-methyl-lactate, respectively. The disparate adsorption amount demonstrated the significant enantioselective adsorption of SURchirMOF-4 for one enantiomer of methyl-lactate. The ee of D-SURchirMOF-4 and L-SURchirMOF-4 for methyl-lactate was 26% and 28%, respectively. Based on the results, SURchirMOF-4 exhibited good enantioselective adsorption toward D/L-methyl-lactate enantiomers.

For the first time, Bräse and colleagues reported a planar-chiral building block employed for CMOFs in which 4,7-disubstituted paracyclophane, a planar-chiral linker, directly integrated into a CMOF and exhibited its application in an enantioselective QCM sensor [76]. A thin film of smooth SURMOF Zn(PcTPDC) was fabricated by a similar

LPE growth strategy on the QCM substrate for the chiral determination of limonene. An achiral SURMOF Cu(DMTPDC) was employed as a seeding layer to assist the growth and improve the crystallinity of chiral Zn(PcTPDC). According to the obtained results, the combination of the chiral features of the planar linker and the porous structure of the MOF showed the chiral character and function, as well as a selective enantioadsorption for racemic nonpolar limonene. To guarantee the reproducibility of the results, the (S)- or (R)-limonene uptakes were studied three times. The average uptake of (S)-limonene was 0.024 ± 0.003 g per g SURMOF, while it was 0.041 ± 0.004 g R-limonene per g SURMOF. Therefore, the ee of R vs. S was 26%. In the same period, Yan and co-workers designed a 3D porous CMOF ($\text{Zn}_2(\text{bdc})(\text{L-lac})(\text{dmf})\cdot\text{DMF}$)-coated QCM sensor for the enantioselective recognition of three pairs of amine enantiomers and one pair of alcohol enantiomers [72]. Otherwise, an easy drop-coating strategy is used for coating the gold surface of quartz crystal with a homogeneous and dense chiral thin film of ($\text{Zn}_2(\text{bdc})(\text{L-lac})(\text{dmf})\cdot\text{DMF}$). The chiral selectivity factors of the developed QCM sensor for S/R-1-(1-naphthyl)ethylamine and S/R-1-phenylethylamine were 1.36 and 2.20, respectively. An increment in the analyte concentration led to an increase in the selectivity factor, while the temperature rise caused its decrease. The proposed method underlined CMOFs' potential as unique sorbents for QCM sensors.

Recently, Xie and colleagues prepared a pair of chiral UiO-MOF-based QCM sensors to effectively recognize Cys enantiomers [77]. The post-modification of UiO-66-NH₂ with tartaric acid enantiomers resulted in the preparation of the D- and L-UiO-tart (chiral UiO-MOF enantiomers). Coating chiral UiO-MOF onto the gold surface resulted in the development of two enantioselective QCM sensors (D- and L-UiO-tart@Au). The UiO-tart coating layer served the role of a chiral selector for the enantioselective adsorption of a Cys enantiomer. The reaction between the Au layer and captured Cys enantiomer led to the significant mass growth of the whole system. Applying the QCM technique allowed the monitoring of the gravimetric alteration of the system and, consequently, the enantioselective distinguishing of Cys. The enantioselective factor (ef) refers to the division of the value of the preferential uptake by the other. Preferential uptakes of L-Cys by L-UiO-tart@Au had a 5.9 ± 0.54 efL value, while the enantioselective adsorption preference of D-UiO-tart@Au became D-Cys and provided a 5.63 ± 0.73 efD value. On the contrary, race-UiO-tart@Au showed an efL value of 1.01 ± 0.08 , meaning there was an equal uptake of D- and L- enantiomers without any obvious enantioselectivity. The results confirmed the chiral sensing performances of D- and L-UiO-tart@Au. In 2021, Heinke et al. developed an enantioselective electronic nose (e-nose), an artificial nose based on QCM sensors coated with six types of nanoporous achiral and homochiral MOF thin films [78]. SURMOFs were fabricated using the layer-by-layer method to prepare MOF thin films on the QCM sensors directly. The e-nose was used for the examination of five pairs of chiral odor molecules: (R/S)-1-phenylethanol, (R/S)-limonene, (R/S)-1-phenylethylamine, (R/S)-2-octanol, and (R/S) methyl lactate, totally 10 volatile organic compounds. Each chiral film enabled discrimination between the chiral odor molecules enantiomers based on providing diverse feedback for each enantiomer. The achiral MOF film coated QCM sensors achieved similar responses for isomers of one chiral odor molecule. In contrast, the homochiral MOF film coated sensors exhibited disparate responses to various enantiomers. The developed CMOF e-nose shows the potential of enantioselective discrimination of chiral odors and is a powerful strategy for improved odor sensing.

5.4. Electrochemical Enantioselective (Bio)Sensor

Electrochemical (bio)sensors have attracted researchers' attention to detect diverse compounds. Compared with other methods, the cardinal virtues of electrochemical (bio)sensors to be extolled are their high sensitivity and reliability, capability of a simple combination with different sensing platforms, low cost, and simple operation [48]. Other merits of this type of biosensor are low specimen need, portability, and ability to be miniaturized. Based on the type of transducer used, electrochemical biosensors are classified as

voltammetric, impedimetric, amperometric, conductometric, or potentiometric. Voltage, potential, and current in the transducer system are all affected by redox processes [79]. Lately, electrochemical (bio)sensing platforms have been used for the enantioselective sensing of chiral compounds [48]. Most enantioselective electrochemical recognition platforms depend on supporting electrodes coated with a chiral interface, termed chiral sensors. The most crucial step in constructing chiral electrochemical (bio)sensors is to fabricate a chiral surface possessing recognition sites; therefore, the conformation of chiral selectors serves a determinant role in the preparation of chiral interfaces [80]. Various chiral interfaces have been generated to fabricate chiral (bio)sensors for enantioselective recognition. In general, in the light of interactions between chiral enantiomers and selectors, electrochemical enantiomer sensing can be chiefly categorized into chiral ligand exchange recognition, host-guest recognition, chiral biological macromolecule adsorption recognition, molecularly imprinted recognition, and MOFs that exhibit excellent performance in electrochemical sensing [80].

In recent years, MOFs have drawn much attention for their exploitation in electrochemical (bio)sensors. MOFs with ultrahigh porosity, surface area, unparalleled tunability, and simple modification offer a novel opportunity to generate 3D cavities as host matrices that can catalyze targets or load guest molecules for sensitive electrochemical detection [81]. Thus, MOFs introduce redox and catalytically active sites from ligands or metal ions, which are beneficial for electrochemical (bio)sensors. However, since most MOFs do not have chemical stability in water and most electrochemical sensing platforms need aqueous electrolytes, the water-stable MOFs become a primary concern for their application in electroanalysis. MOF structures are generally vulnerable to water molecule attacks, resulting in phase shifts, ligand displacement, and structural disintegration. A water-stable MOF structure must be robust enough to prevent water molecules from entering the framework and causing crystallinity and overall porosity losses. MOF structures with high stability often include vigorous coordination bonds (thermodynamic stability) or considerable steric hindrance (kinetic stability) to avoid the harmful hydrolysis process that destroys the metal-ligand interactions [82]. Furthermore, MOFs have conventionally been believed to be poor electrical conductors because of their ligand-insulating properties. Consequently, several studies have introduced other mechanically durable and highly conductive substances in MOFs to overcome drawbacks, such as low electronic conductivity, poor water stability, and inadequate electrocatalytic potential. Meanwhile, some MOFs demonstrate good electrochemical activity for designing unique electrochemical (bio)sensors if organic linkers and metal ions are included [83,84]. With a better knowledge of the structural stability of MOFs in water systems and ongoing efforts, the number of research papers on water-stable MOFs is increasing, and many more are published yearly [82]. An early report on integrating MOFs into electrochemical sensors was done by Shi et al. in 2017, in which they synthesized a new guest-free homochiral MOF $(\text{Cu}_4\text{L}_4)_n$, where $\text{L-H}_2\text{L}$ (N-(2-hydroxybenzyl)-L-leucine) was used as a starting material [85]. The synthesized CMOF showed excellent stability in water and air. Then, an enantioselective electrochemical sensor was fabricated by the direct modification of a glass carbon electrode (GCE) with $(\text{Cu}_4\text{L}_4)_n$ nanocrystals without further post-modification and desolvation for the recognition of α -methylbenzylamine (MBA) enantiomers. The developed CMOF-modified electrochemical chiral sensor exhibited great electro-conducting properties and specific oxidation signals for S(-)/R(+)- α -MBA enantiomers with a detection limit of 1.3 μM and a 0.002 to 0.1 mM concentration range. The $(\text{Cu}_4\text{L}_4)_n$ nanocrystals-based electrochemical sensor showed the capability of enantioselective discrimination and enabled the fast quantitative recognition of ee in the mixture of chiral amine.

In the same period, Li and colleagues employed a combination of β -cyclodextrin (β -CD) and MOF for developing a molecularly imprinted electrochemical sensor for the enantioselective determination of L-phenylalanine (L-Phe) for the first time [86]. Gold-thiol chemistry was employed for functionalizing gold nanoparticles (Au NPs) by L-Cys and thiolated β -cyclodextrin to serve as a basis for the microporous MOF formation. Preparation of the molecularly imprinted-MOF (MI-MOF) was done by depositing the functionalized

Au NPs through electropolymerization in the existence of L-Phe and 4-aminothiophenol as a template molecule and functional monomer, respectively (Figure 7). During the enantiomeric recognition procedure, the phenyl ring of L-Phe integrated into cyclodextrin's hydrophobic cavity, while L-Cys captured the other end of L-Phe through electrostatic interaction. The imprinted electrochemical sensor indicated great enantiomeric selectivity and high precision with a 0.33 pM LOD for recognition to L-Phe.

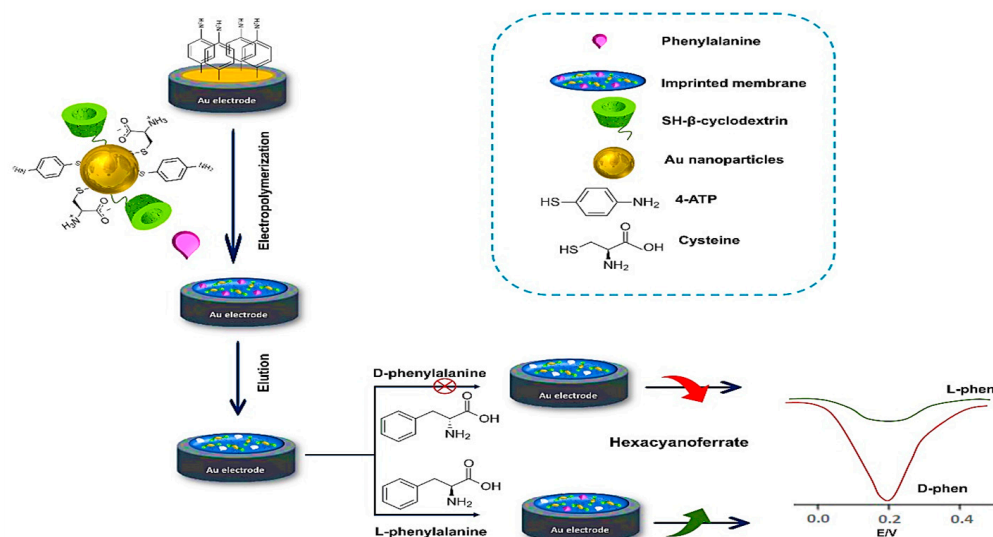


Figure 7. Fabrication procedure of the microporous MI-MOF-based enantioselective electrochemical sensor for recognizing L-phenylalanine enantiomers [78]. Redrawn by PowerPoint 365 software.

In 2021, Liu et al. designed a highly selective and efficient electrochemical sensor based on the integration of CMOFs with a multi-walled carbon nanotube (MWCNT) for the sensitive chiral sensing of D/L-Trp [87]. Several MOFs were synthesized in various conditions to achieve electrochemical chiral determination. For the enantio-specificity, different amino acids were introduced into the MOFs' skeletons using the hydrothermal technique. Figure 8 shows an experimental process of grain-like L-Phe-MOF (grain-CMOF) synthesis by adding L-Phe to inorganic metals ($\text{CuSO}_4 \cdot 3\text{H}_2\text{O}$) and organic ligands. Integrating the CMOF with MWCNT resulted in a functional electroensing interface with enhanced conductivity. The enantioselective determination of D/L-Trp with a linear range between 0.4–19 μM and a detection limit of 0.16 μM for D-Trp and 0.11 μM for L-Trp was obtained by an MCNT/CMOF-based electrochemical sensor. The prepared sensor exhibited remarkable selectivity and reproducibility for recognizing Trp enantiomers.

Kuang and co-workers recently developed an enantioselective electrochemical sensor with two chiral sites, including a chiral skeleton for self-assembled CMOF (Ca-sacc/MeOH) and a chiral cavity for β -CD based on the electrochemical oxidation of β -CD onto Ca-sacc/MeOH [88]. The designed multi-chiral β -CD@Ca-sacc/MeOH-modified GCE was employed for the simultaneous enantiomeric recognition of penicillamine (Pen) and Trp. According to the achieved results, the linear range for D/L-Trp and D/L-Pen was 0.01 to 0.5 mM, and the low limits of detection were 0.23 μM for D-Trp, 0.098 μM for L-Trp, 0.79 μM for D-Pen, and 0.18 μM for L-Pen, respectively. The prepared β -CD@Ca-sacc/MeOH-based chiral sensor demonstrated excellent chiral recognition capability of the isomers D/L-Pen and D/L-Trp, as well as high stability and repeatability. Combining multi-chiral sources is essential for constructing unique platforms for the simultaneous chiral recognition of two distinct compounds. In 2022, Wang et al. reported a new MOF (Phe-Cu-PTA) structure that was fabricated by the organic ligands (1.10-Phe [pheanthroline], PTA [terephthalic acid]) and metal ion Cu^{2+} , which were applied to differentiate D/L-Trp enantiomers [89]. The excellent chiral recognition selectivity and sensitivity realization were made possible by successfully combining the two organic monomers with Cu^{2+} . Phe-Cu-PTA is securely

anchored on GCE as an electroensing interface to overcome the instability of MOF material in high humidity or aqueous environments. Due to the various steric configuration of the D/L-Trp enantiomers, MOFs (host)-Trp enantiomers (guest) interactions are different for D- and L-Trp. Peak currents steadily rose with increasing concentrations of D-Trp or L-Trp, as the concentration of Trp increased from 1 mM to 6 mM. Trp-enantiomers D-Trp and L-Trp had detection limits of 0.34 M and 0.12 M, respectively. Therefore, based on the results of the proposed MOF, Phe-Cu-PTA exhibited a considerably greater binding force toward D-Trp than L-Trp and achieved significant enantioselectivity efficacy.

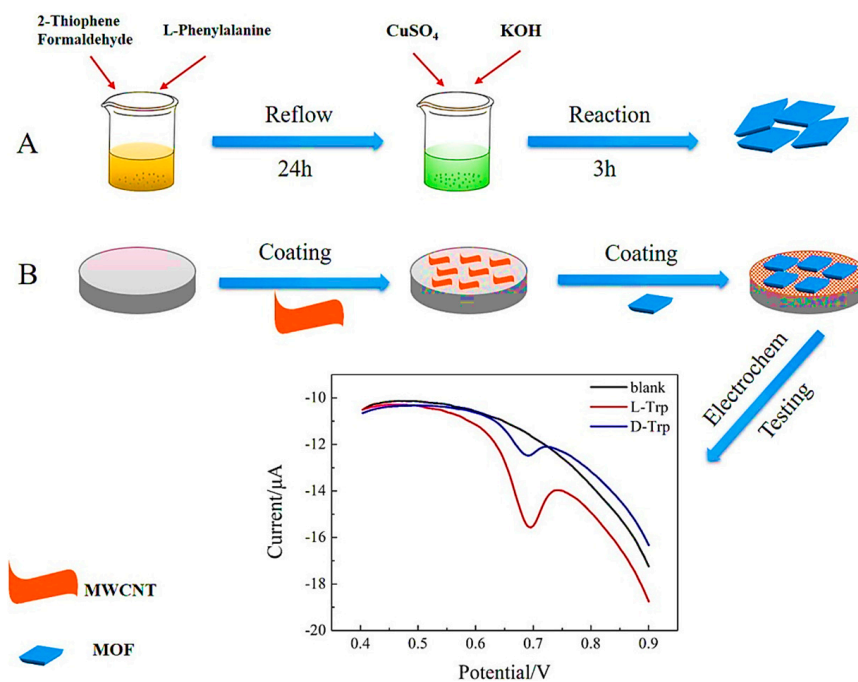


Figure 8. Representation of grain-CMOF/MWCNT interface for electrochemical enantio recognition of tryptophan. Reprinted (adapted) with permission from [87].

In the same year, Wang and colleagues synthesized a CMOF (D-His-ZIF-8) by a one-pot method through the in situ exchange of 2-methylimidazole on ZIF-8 with D-His for the development of a chiral electrochemical sensor [90]. Introducing Ketjen Black (KB) to the D-His-ZIF-8 electroensing interface as a conductive substrate substance enhanced the conductivity of the CMOF (Figure 9). The chiral electrochemical sensor indicated that KB/D-His-ZIF-8 had the potential for the enantioselective recognition of amino acids. Trp enantiomers exhibited the highest recognition efficiency. Trp's higher recognition effectiveness (5.78) compared to other amino acids can be attributed to its relatively larger size. Based on the mechanism of enantiomeric recognition, the binding of D-His-ZIF-8 with an L-amino acid resulted in the determination of chiral molecules of various configurations. According to the results, the enantiomer recognition ability of the KB/D-His-ZIF-8/GCE for D/L-Trp showed a linear range between 0.01 and 5.0 mM with detection limits of 0.23 μ M for D-Trp and 0.51 μ M for L-Trp. This study paves the way for developing chiral electrochemical sensing platforms based on D-His-ZIF-8.

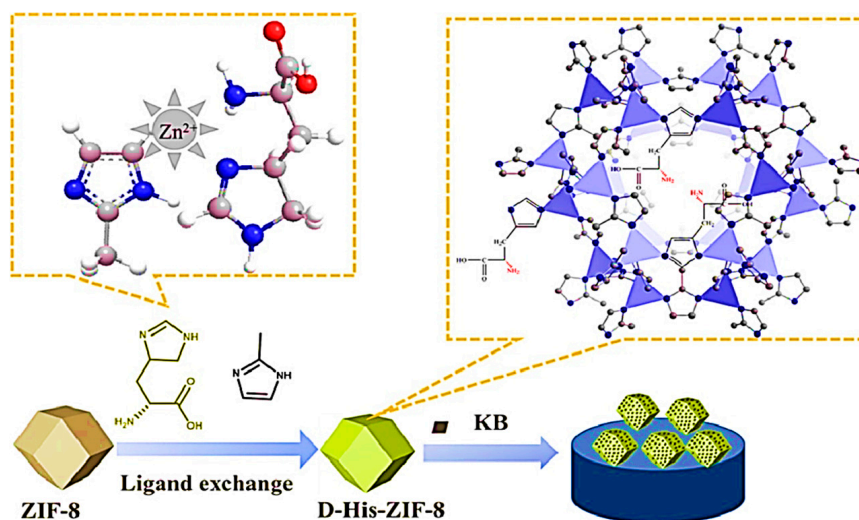


Figure 9. Scheme of the fabrication of D-His-ZIF-8-based enantioselective electrochemical sensing platform. Reprinted (adapted) with permission from [90].

In another study, Cai et al. reported the successful preparation of the L-His-ZIF-8 CMOF for the enantiodiscrimination of Tyr and Trp isomers via a two-step electrodeposition technique by utilizing L-His as a chiral selector [91]. The L-His-ZIF-8-based electrochemical chiral sensor recognized the Trp and Tyr isomers. Still, interestingly, they exhibited contrasted voltammetric behavior on the differential pulse voltammograms (ID-Tyr > IL-Tyr, whereas ID-Trp < IL-Trp), which was described by the density functional theory (Figure 10). Subsequently, to achieve the highest determination efficacy of the L-His-ZIF-8-modified GCE toward the Tyr and Trp isomers, both the electrodeposition time and the pH were optimized. However, the isomers of both amino acids were successfully differentiated with the designed electrochemical chiral sensor. Still, the sensor could only be recognized at the mM level because of the insufficient conductivity of synthesized CMOF ZIF-8. Table 1 shows a summary of MOF-based enantioselective sensors. Table 1 shows a summary of MOF-based enantioselective sensors.

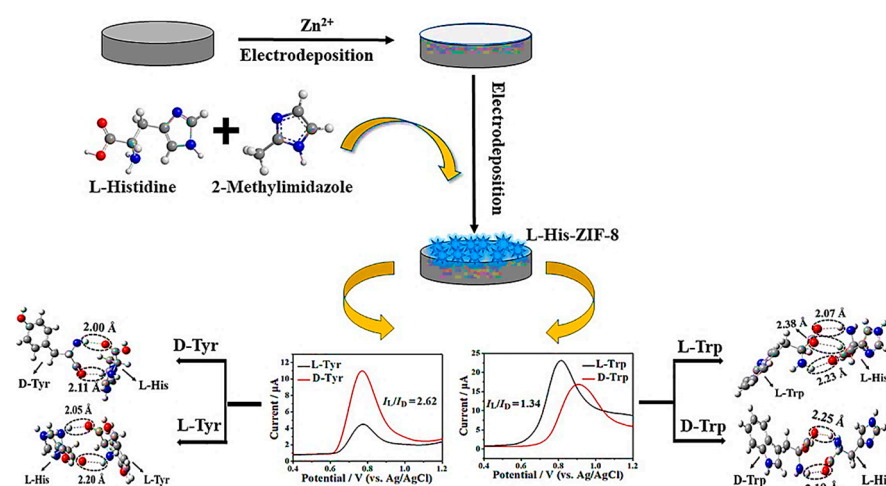


Figure 10. Schematic representation of preparation procedure of L-His-ZIF-8/GCE for electrochemical chiral sensing and of tryptophan and tyrosine isomers. Reprinted (adapted) with permission from [91].

Table 1. Analytical performances of MOF-based enantioselective sensors.

MOF Formula	Analytes	Transduction Type	LOD	Linear Range	Ref.
MPA ¹ -capped CdTe QD ² @MOF	D/L-tartaric acids, D/L-dimethyl tartrates, D/L-mandelic acids	Fluorescence	-	30–500 µg/mL	[92]
{[Cd(L)(4,4'-bipy)]·DMA·5H ₂ O} _n	D/L-penicillamine	Fluorescence	0.9 µM (D-Pen) 2.1 µM (L-Pen)	20–167 µM	[93]
IRMOF ³ -74-I/II-Mg-C-Tb	Phenylethanol, phenethylamine, cinchonine and cinchonidine, and N- benzylcinchoninium chloride and N- benzylcinchonidinium chloride	Fluorescence	-	0.01–17 mM	[94]
Single-crystalline 2D MONs ⁴	α-pinene, limonene, β-pinene, valencene, and isolongifolene	Fluorescence	-	0–175 µM	[95]
3D layered porous MOF	Alaninol, leucinol, phenylalaminol, and phenylglycinol	Fluorescence	-	30–150 µL	[96]
S-1 (L-AP@UiO-66-(COOH) ₂) and R-1 (D-AP@UiO-66-(COOH) ₂)	L/D-amino propanol	Fluorescence	-	10 ⁻⁴ –10 ⁻² M	[97]
Helical-Ag NPs @ MOF	D/L-cysteine and D/L-asparagine	Fluorescence	-	1.0 µM	[98]
2D HMOF-3 nanosheets (HMOF-3-NS)	R/S-mandelic acid, D/L-tartaric acid, D/L-lactic acid, D/L-alanine, and D/L-tryptophan	Fluorescence	-	0–50 µM	[99]
nanorod-shaped homochiral Cd-MOF	D/L-aspartic acid	Fluorescence	-	1 nM	[100]
Zr-MOF	D/L-glutamine (Gln)	Fluorescence	D-Gln 6.6 × 10 ⁻⁴ M and L-Gln 3.3 × 10 ⁻⁴ M	10–100 µM	[101]
[Zn(L)(2,2'-bipy)]·H ₂ O (LNNU-1)	Tryptophan	Fluorescence	1.94 µM (L-Trp), 2.59 µM (D-Trp), 1.91 µM (DL-Trp)	0–0.125 mM	[71]
Ru (ruthenium)-MOF	Tryptophan	Electrochemical	0.33 nM	1.0 nM–1.0 mM	[102]
CD (cyclodextrin)-MOF	α/β-Pinene	Electrochemical	-	0.5–5.0 mM	[103]
MOF@CCQDs/NiF ⁵	D/L-Tyrosine	Electrochemical	6.12 × 10 ⁻⁶ M (D-Tyr) 9.85 × 10 ⁻⁷ M (L-Tyr)	0.2–1.2 mM	[104]
h-HDGA@ZIF-67	Penicillamine (Pen)	Electrochemical	0.022 µM (L-Pen) 0.015 µM (D-Pen)	3.25–19.50 mM	[105]
TiO ₂ /MIL-125-NH ₂ NTs	3,4- dihydroxyphenylalanine (L/D-DOPA) enantiomers	Electrochemical	0.24 µM	1.0–10.0 µM	[106]
AChE ⁶ /L-Ni-BPY/DpAu/GCE	Galantamine hydrobromide	Electrochemical	0.31 pM	1 × 10 ⁻¹² –1 × 10 ⁻⁶ M	[107]
C-dots@MOF/CuF	Penicillamine	Electrochemical	-	100–600 µM	[108]
L-His-ZIF	D/L-Glutamate	Electrochemical	0.06 nM	0.1–50 nM	[109]
Cu-MOF: {[Cu(fdc)(bpe)(H ₂ O)(DMF)]·0.5H ₂ O} _n	L-Tryptophan	Electrochemical	5.822 µM	0.01 to 0.09 mM	[110]

¹ Mercaptopropionic acid. ² Quantum dot. ³ Isoreticular MOFs. ⁴ MOF nanosheets. ⁵ Chiral carbon quantum dots on Ni foil. ⁶ Acetylcholinesterase.

6. Metal–Organic Frameworks as Chiral Stationary Phases for Chromatographic Enantioseparation

By considering the significance of enantioseparation, scientists have devoted much time and energy into developing CMOF-based separation techniques. Among all the enantioseparation methods, chromatographic separation on CSPs has been widespread because of its high effectiveness in the enantiomeric purity measurement and racemates separation [111]. During the last few years, MOFs have been investigated as new CSPs for chromatographic separations, but more recently, CMOFs' utmost potential for the enantioseparation of racemic mixtures using chromatographic techniques has been inspired due to their enantioselective adsorptive separation abilities [112]. Therefore, MOFs with overall stability, intrinsic chiral activity, structural diversity, ease of fabrication, and selective adsorption capability based on physical coating or chemical bonding are ideal CSP candidates in HPLC, GC, and CEC [113].

6.1. High-Performance Liquid Chromatography Chiral Separation

High-performance LC is well-known as the most effective and fastest chromatographical technique. With the expansion of CMOFs for enantioseparation, there are more researchers who prefer using HPLC for enantioselective separations compared to GC because the chiral recognition mechanism is mainly related to the liquid phase [114]. The significant dissimilarity between GC and HPLC is that GC utilizes a gaseous mobile phase and liquid stationary phase, whereas HPLC employs a liquid mobile phase and solid stationary phase. Moreover, high-performance LC can deal with most soluble materials despite their volatility while also analyzing volatile compounds. This feature immensely broadens the operational capacities of HPLC compared to those of GC [114]. CMOFs have become one of the most stunning chiral separation materials for HPLC due to their homogeneous structural cavities, superior thermal and chemical stabilities, large surface area, and selective enantioseparation of racemic mixtures. Direct packing of MOFs with broad size distributions, sub-micrometer sizes, and irregular forms results in unfavorable peak morphologies, inefficient separations, and excessive column backpressures. As a solution, a layer-by-layer deposition technique can be used to regulate the growth of thin films of MOF onto core-shell silica particles [115].

The first analytical approaches based on applying MOFs as CSPs for chromatographic separation or as sample preparation materials usually depend on the direct packing of MOFs into the HPLC column. MOFs' unique pore structure paves the way for separating structurally similar substances like positional isomers. This novel selectivity is assigned to the combination of adsorption and molecular sieves effects [116]. Nonetheless, the critical limitations of these packaging include the requirement for high mobile phase pressure and low column efficiency due to the irregular forms of packing crystals. To solve these problems and reduce limitations, core-shell MOF-based compounds have emerged as alternative materials for chromatographic separation. The core-shell MOF-based compounds as HPLC stationary phase hydrophilic and mixed modes have superior attributes compared to single MOF materials with low column efficiency and high column pressure dilemmas. The advantages and disadvantages of each HPLC column are shown in Figure 11 [116].

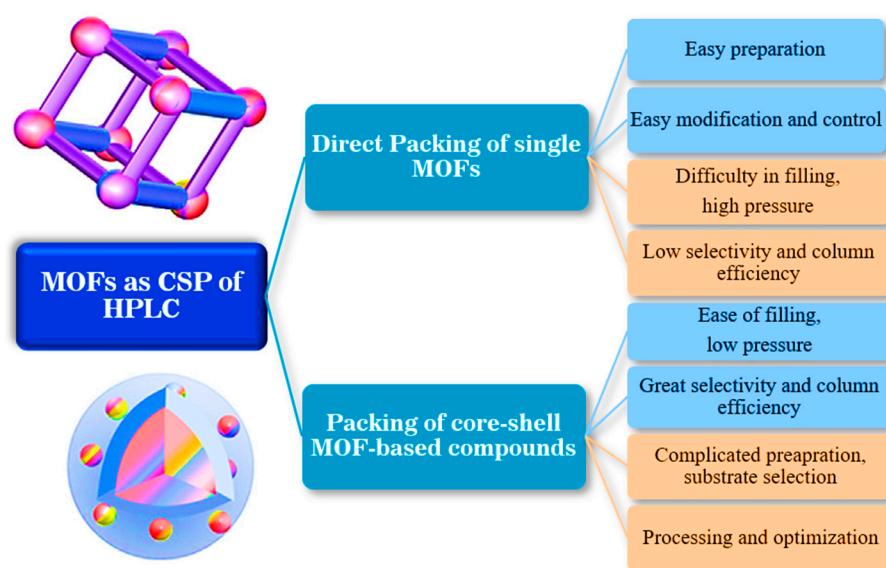


Figure 11. The pulse points and downsides of core-shell MOF and single MOF particle-based composites employed as HPLC columns.

In 2007, Fedin and colleagues reported the first successful liquid chromatographic determination of enantiomers by utilizing a homochiral Zn-organic framework as a CSP [117]. They managed to package a pre-established CMOF into a chromatographic column for the enantiomeric separation of many sulfoxides. Only methyl phenyl sulfoxide (PhSOMe), one of the sulfoxides, had baseline separation. In contrast, the addition of any substituents in the aromatic ring caused a reduction in both enantioselectivity and the sorption constant. This pioneering research verified the possibility of CMOFs as a chiral stationary phase for enantioselective HPLC separation.

It was not until five years later, in 2012, that another example of employing a CMOF as a CPS for enantioselective high-performance liquid chromatographic separation emerged. Tanaka et al. synthesized a homochiral (R)-MOF-silica composite to use as a CSP for the selective enantiomeric resolution of different sulfoxides (phenyl methyl sulfoxide, *o*-MePhSOMe, *p*-MePhSOMe, *p*-MeOPhSOMe, *m*-ClPhSOMe, *p*-ClPhSOMe, *p*-NO₂PhSOMe, *o*-MeOPhSOMe, *o*-ClPhSOMe, phenyl vinyl sulfoxide, benzyl methyl sulfoxide, benzyl phenyl sulfoxide, naphthyl methyl sulfoxide, and dialkyl sulfoxides) [118]. The enantiomeric separation was examined using two eluents. Fortunately, 9 out of 16 types of sulfoxides showed complete enantioseparation by utilizing Eluent I (hexane-EtOH (50/50)) as the mobile phase. However, the other two were efficiently separated by the less polar Eluent II (hexane-EtOH (50/50)), and the rest of the sulfoxides demonstrated the poor separation of their enantiomers in both solvent systems. This result may be a promising future for CMOF compounds in the enantioselective separation of different chiral substances. Considering CMOFs' outstanding performance, Cui et al. employed two isostructural 1,1'-biphenol-based CMOFs decorated with chiral dimethoxy or dihydroxyl groups, including 1D-nanosized channels [46]. The chiral dihydroxyl-group-decorated framework serves the role of the chiral stationary phase of HPLC for the enantiomeric resolution of racemic amines with high enantioselectivity and as a solid-state host, which can adsorb and resolve racemic aromatic and aliphatic amines. The present adsorption separation technique was employed for the enantioseparation of racemic 1-phenylethylamine. Experimental results and molecular simulations reveal that the inherent chiral identification and separation referred to the various orientations of enantiomers and their binding energies in the microenvironment of the CMOF.

In 2014, Tang and co-workers developed a 3D-molecular sieve-like homochiral CMOF, [(ZnLBr)·H₂O]_n [119]. The synthesized 3D-CMOF was employed as a CSP for HPLC to the enantiomeric resolution of racemic drugs, including ibuprofen, phenylethylamine,

phenyl-1-propanol, and benzoin, with molecular sieving performances based on the relative sizes of the resolved molecules and the chiral channels. The molecular sieve-like CMOF-packed column showed excellent efficiency in the enantioseparation of the racemic mixtures with a minimum kinetic diameter (MKD) and gave baseline separation (Figure 12). Racemic naproxen and ketoprofen did not exhibit enantioseparation despite having close minimum kinetic diameters (9.7 and 9.4 Å, respectively) to chiral channels (~9.8 Å). This suggests that they could not penetrate the interior of the chiral pores to exhibit a molecular sieve-like manner.

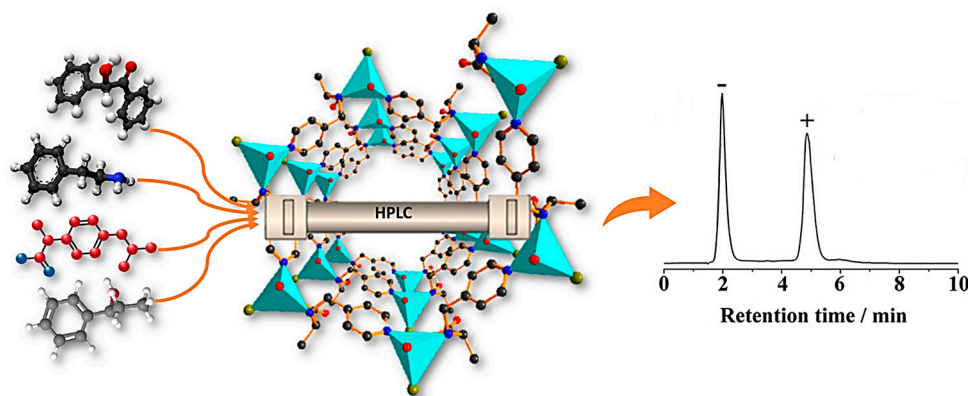


Figure 12. Enantioselective separation of four types of racemic compounds by HPLC through using 3D-molecular sieve-like homochiral CMOF. Injected mass: 20 µg of each racemate. UV detector, hexane/isopropanol as the mobile phase. Reprinted (adapted) with permission from [119]. Copyright 2014 American Chemical Society and redrawn with PowerPoint 365 software.

In 2016, Stoddart and colleagues reported a novel, renewable, and green CMOF consisting of γ -cyclodextrin (γ -CD) and alkali metal salts, termed CD-MOF, that accomplishes the efficient HPLC separation of a broad range of mixtures, such as ethylbenzene from styrene, haloaromatics, terpinenes, pinenes, four isomers, and other chiral compounds [120]. It should be noted that each γ -CD torus has 40 stereogenic centers, which can lead to the enantioselective recognition of each pinene regioisomer. The capability of CD-MOF to operate as a separation phase for a broad spectrum of materials, such as vinyl-, alkyl-, haloaromatics, unsaturated and saturated alicyclic substances, and chiral composites, differentiated it from most other frameworks utilized as CSPs in separations. Considering that the CD-MOF is a homochiral MOF, it can enhance the enantiomeric resolution of chiral analytes involving those of 1-phenylethanol and limonene. These CD-MOFs-based stationary phases could be low-cost and simple for preparation in comparison to other CSPs, including CD-bonded silica particles. In addition to the great properties of CMOFs in chiral separation, the non-uniformity and irregular morphology of synthesized MOFs lead to increased column backpressure and decreased column efficacy for MOF-packed columns, which considerably influences their performance for separation.

In later years, Zhang and co-workers demonstrated the effective one-pot technique for immobilizing CMOF [Cu₂((+)-Cam)₂Dabco] (Cu₂C₂D) onto silica microspheres or, in other words, the layer-by-layer growth coating method of Cu₂C₂D on microspheric SiO₂ [121]. Finally, a uniform SiO₂@CMOF@CMOF core-shell-microsphere was generated as a chiral stationary phase for HPLC (Figure 13). Controlling the [Cu₂((+)-Cam)₂Dabco] growth cycles led to the reasonable regulation of column efficiency and shell thickness. The separation performance improved with the increment of the CMOF's growth cycles. Based on the mechanism of chromatographic separation, such as hydrogen and hydrophobic bonding, the developed CSP successfully separated various racemic substances, including labetalol hydrochloride, malic acid, and indole derivatives, under normal phase LC conditions. The RSD of retention time was less than 1.1%, demonstrating the good stability and repeatability.

bility of the chiral $\text{SiO}_2@Cu_2C_2D-2$ column for chiral separation by HPLC. Moreover, the $\text{SiO}_2@Cu_2C_2D-2$ -packed column exhibited high column efficacy and low back pressure.

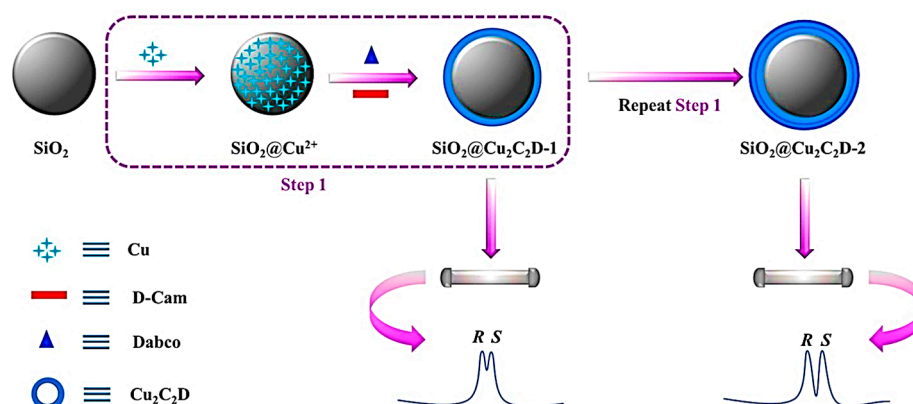


Figure 13. Schematic illustration of the fabrication process of $\text{SiO}_2@Cu_2C_2D$. Reprinted (adapted) with permission from [121].

In 2020, Yuan et al. synthesized homochiral CMOF@ SiO_2 core-shell microspheres, named D-His-ZIF-8@ SiO_2 , as a CSP of HPLC for the enantioseparation of 18 racemates with different structures (phenol, alcohol, organic acid, ketone, and amine) [122]. As a chiral ligand, D-His was embedded in the ZIF-8 framework. The D-His-ZIF-8 was a suitable silica-based core-shell compound because of its excellent features, including a simple synthesis process, nano-scale size of crystal particles, ease of surface modification, and stability of the framework structure. Although the L-his-ZIF-8@ SiO_2 -packed column showed results for the chiral separation of the racemates, the D-his-ZIF-8@ SiO_2 -packed column demonstrated high enantioselectivity, great resolution for racemates, and complementary to the commercial Chiralpak AD column. Therefore, the D-His-ZIF-8@ SiO_2 -packed column exhibited good stability, reproducibility, and great resolution potential for the efficient and fast HPLC chiral separation of a variety of racemates. The D-his-ZIF-8@ SiO_2 column showed 0.89% RSD of the retention times through repetitive analyte separation (50th, 100th, 150th, 200th, and 250th injections). Thus, fabricating CMOF@ SiO_2 core-shell microspheres is an efficient method for improving homochiral CMOFs application as CSPs in the chromatographic techniques.

By extension of the valuable methods for the fabrication of CMOFs for improved chiral HPLC separation, Cui and co-workers were the first to demonstrate the highly stable and robust Zr(IV)-based CMOFs as an efficient CSP for reversed-phase HPLC (RP-HPLC) [123]. These Zr(IV)-based CMOFs could obtain exceptional enantioseparation of a wide range of N-containing drugs and amino acids under acidic aqueous eluent conditions. Crown ether-modified bisphenol scaffolds were used for the reticular synthesis of a series of these MOFs (Figure 14). The performance of Zr(IV)-based CMOF-packed columns were evaluated after 1 year of shelf life and more than 4000 injections, which shows its good durability. The separation performance decreased with reduced α/R_s from 5.25/6.31 \rightarrow 4.23/3.93. The RSDs of peak area, selectivity factor, theoretical plate number, and peak height were <2.0%, confirming the stability of the Zr-CMOF-packed column. The Zr-CMOF-packed HPLC columns rendered high selectivity, resolution, and durability for the enantioseparation of various racemates. The density functional theory calculations propose that Zr-based CMOF offers a confined space for combination with chiral crown ether moieties devoted to the selectivity of separation. This research draws attention to the distinctive potential of robust MOF decoration with chiral crown ether functional groups to ease the RP-HPLC separation of effective racemic pharmaceuticals and chemicals.

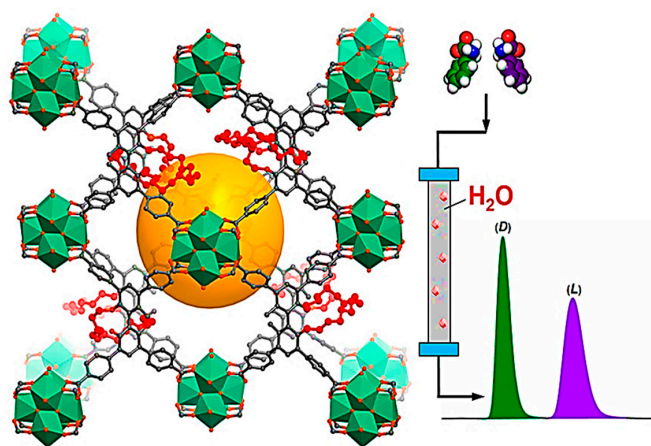


Figure 14. Enantioselective RP-HPLC separation of chiral compounds with robust Zr(IV)-based CMOFs. Reprinted (adapted) with permission from [123]. Copyright 2021 American Chemical Society.

In 2021, Yuan and colleagues were the first to employ a post-modification strategy for the modification of an achiral MOF (MIL-101) surface by utilizing chiral polyaniline (c-PANI) for the synthesis of a chiral MIL-101@c-PANI core-shell material, which was employed as an HPLC stationary phase for enantiomeric resolution (Figure 15) [124]. The MIL-101@c-PANI column provided good resolution with baseline separation for 1,2-diphenyl-1,2-ethanediol, 3-(benzyloxy)-1,2-propanediol, ketoprofen, and amlodipine. 3-(Benzyloxy)-1,2-propanediol had the highest resolution value of 3.35. The MIL-101@c-PANI-packed column separated a broad range of chiral compounds, such as ketones, alcohols, aldehydes, esters, amines, and organic acids, with good enantiomer resolution potential. The separation factors of most of the racemates on the MIL-101@c-PANI-packed column were higher than the commercial tris(3,5-dimethylphenylcarbamoyl) amylose-packed column. In addition, the commercial tris(3,5-dimethylphenylcarbamoyl) amylose-packed column was unable to separate 2-phenylpropanal, ofloxacin, and 1-(1-naphthyl) ethanol, while the MIL-101@c-PANI-packed column could. Additionally, the designed stationary phase exhibited great selectivity for the positional isomers' separation, such as dinitrobenzene and toluidine. The MIL-101@c-PANI compound increased the synergistic effect by integrating the benefits of MIL-101 and c-PANI, which is suitable for improving the enantiomer resolution performance. The RSDs of the retention times for praziquantel and 1,2-diphenyl-1,2-ethanediol after the 50th, 100th, 150th, 200th, and 250th injections were 0.28 and 0.59%, respectively. Their retention times did not significantly alter after hundreds of separations on the MIL-101@c-PANI-packed column, revealing that the MIL-101@c-PANI column had good reproducibility for HPLC separations.

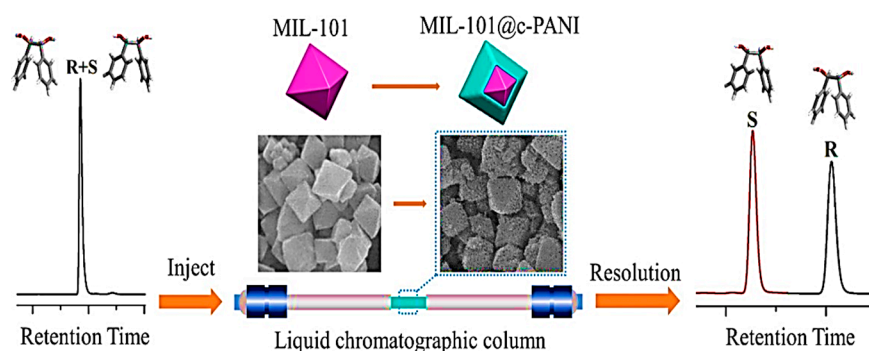


Figure 15. HPLC enantioseparation based on the application of chiral polyaniline-modified MOF core-shell composite MIL-101@c-PANI. Reprinted (adapted) with permission from [124].

For the first time in 2022, Ouyang and colleagues developed a rapid strategy to achieve the unusually spherical crystal morphology of Co-MOF-74 with a size of around 5 μm by adjusting the ratio of reactants, synthetic pathway, temperature, and the amount of 2-methylimidazole (2-MI) [125]. Then, they integrated L-Tyr into the Co-MOF-74 parent framework through an easy, green PSM method for functionalizing the Co-MOF-74 with L-Tyr, termed Co-MOF-74-L-Tyr crystal, in water to make a chiral microenvironment. The Co-MOF-74-L-Tyr-packed column exhibited increased column efficacy and declined back-pressure. The developed homochiral Co-MOF-74-L-Tyr CSP showed excellent enantiomeric resolution for eight drug racemates and drug intermediates, including benzoin, nimodipine, nitrendipine, bi-2-naphthol, and 2,2'-furoin, under normal phase condition (Figure 16). The remarkable stability and repeatability of the Co-MOF-74-L-Tyr were evaluated by replicating the chiral separation of flavanone and nimodipine. There was no significant change in the retention times and resolutions of the 50th, 100th, 150th, 200th, and 250th injections. The resolutions and retention times' RSD values were 1.12% and 0.85%, respectively. The morphology/size-controlled method paired with the green PSM opens new avenues for fabricating target CMOFs with predesigned functional groups as an efficient complement for the CSPs preparation in chiral chromatographic techniques. Table 2 demonstrates a summary of MOF-based composites as CSPs for racemates resolution by HPLC.

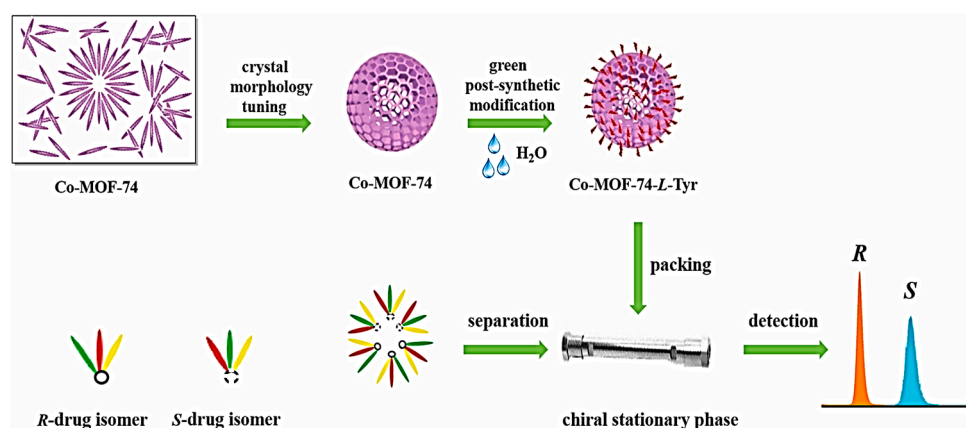


Figure 16. Crystal morphology tuning and post-synthetic modification of Co-MOF-74 for enantioselective HPLC separation of eight drug racemates. Reprinted (adapted) with permission from [125].

Table 2. MOF-based composites used as chiral stationary phases for HPLC.

Type of MOF	Analyte	Mobile Phase	Form	Repeatability (RSD%)	Ref.
(R)-CuMOF-1 and (R)-ZnMOF-1	Sulfoxides, sec-alcohols, β -lactams, benzoin, flavanones, and epoxides	Hexane/EtOH (50/50)	Packing (10 cm length \times 4.6 mm i.d.)	-	[126]
$[\text{Cd}_2(\text{d-cam})_3] \cdot 2\text{Hdma} \cdot 4\text{dma}$ (Cd-MOF)	(\pm)-1-(1-naphthyl)ethanol	Hexane/dichloromethane (1/1)	Packing (25 cm long \times 2.0 mm i.d.)	2.1%	[127]
MOF $[\text{Co}_2(\text{D-cam})_2(\text{TMDPy})]@ \text{SiO}_2$ core-shell composites	Positional isomers (trans-stilbene oxide and phenylenediamine)	n-Hexane/isopropanol (9/1)	Packing (25 cm length \times 2.1 mm i.d.)	0.86% and 0.78%	[128]
$[(\text{CH}_3)_2\text{NH}_2][\text{Cd}(\text{bpdc})_{1.5}] \cdot 2\text{DMA}$	1,1'-Bi-2-naphthol, 1,2-diphenyl-1,2-ethanediol, 1-(4-chlorophenyl)ethanol, furoin, benzoin, flavanone, Troger's base, 3-benzyloxy-1,2-propanediol, 3,5-dinitro-N-(1-phenylethyl)benzamide, and warfarin sodium	Hexane/dichloromethane (2/1)	Packing (25 cm long \times 2.0 mm i.d.)	-	[129]

Table 2. Cont.

Type of MOF	Analyte	Mobile Phase	Form	Repeatability (RSD%)	Ref.
(R)-MOF-4-silica and (R)-MOF-5-silica composites	Sulfoxides, sec-alcohols, and flavanones	Hexane/2-PrOH (90/10)	Packing (10 cm long × 4.6 mm i.d.)	-	[130]
Helical MOF [Zn ₂ (D-Cam) ₂ (4,4'-bpy)] _n (1)	(±)-1-(1-Naphthyl)ethanol, Tröger's base	Hexane and hexane/dichloromethane (95/5)	Packing (25 cm long × 4.6 mm i.d.)	-	[131]
(Me ₂ NH ₂) ₂ [Mn ₄ O(D-cam) ₄ ·(H ₂ O) ₅]	(±)-ibuprofen and (±)-1-phenyl-1,2-ethadiol	Hexane/isopropyl alcohol (96/4)	Packing (10 cm length × 4.6 mm i.d.)	-	[132]
Homochiral MOF [Cu(S-mal)(bpe)] _n	Benzion, propranolol hydrochloride, ketoprofen, DNB-leucine, amlodipine, hydrobenzoin, chlorpheniramine maleate, p-hydroxyphenylglycine, naproxen, furoin, mandelic acid, 1-(9-anthryl)-2,2,2-trifluoroethanol, 1,1'-bi-2-naphthol, praziquantel, ibuprofen, and 1-(1-naphthyl)ethanol	Different ratios of hexane/isopropanol (v/v)	Packing (25 cm long × 2.0 mm i.d.)	1.1%	[133]
γ-CD (cyclodextrin) MOF	Aromatic alcohols	Different ratios of dichloromethane: MeOH and hexane: Dichloromethane (v/v)	Packing (25 cm long × 4.6 mm i.d.)	0.3–0.4%, 1.5–2.1%, and 1.1–1.9%	[134]
[Zn(L-tyr)] _n (L-tyrZn), [Zn ₄ (btc) ₂ (Hbtc)(L-His) ₂ (H ₂ O) ₄ ·1.5H ₂ O, {[Zn ₂ (L-trp) ₂ (bpe) ₂ (H ₂ O) ₂ ·2H ₂ O·2NO ₃] _n , [Co ₂ (L-Trp)(INT) ₂ (H ₂ O) ₂ (ClO ₄)], [Co ₂ (sdba)(L-Trp) ₂] and [Co(L-Glu)(H ₂ O)·H ₂ O] _∞	Alcohols, amines, ketones, ethers, organic acids	Different ratios of hexane/isopropanol or hexane/dichloromethane (v/v)	Packing (25 cm long × 2.0 mm i.d.)	-	[135]
[Cu ₂ (D-Cam) ₂ (4,4'-bpy)] _n	Positional isomers and 1-(9-anthryl)-2,2,2-trifluoroethanol, 1,1'-bi-2-naphthol, flavanone, 2-phenyl-1-propanol, 1-(1-naphthyl)ethanol, and 3-benzyloxy-1,2-propanediol	Hexane/isopropanol (98/2) and different ratios of hexane/dichloromethane (v/v)	Packing (25 cm long × 4.6 mm i.d.)	-	[136]
[Nd ₃ (D-cam) ₈ (H ₂ O) ₄ Cl] _n	Ofloxacin, warfarin, naproxen, furoin, benzoic acid, phenylalanine, glutamic acid, threonine, tyrosine, alanine, cysteine, aspartic acid, valine, histidine, leucine, serine, isoleucine	n-Hexane/isopropanol (9/1), MeCN/H ₂ O (6/4), MeOH/H ₂ O (6/4), ethanol absolute	Packing (25 cm long × 2.0 mm i.d.)	-	[137]
[Co(L)(bpe) ₂ (H ₂ O) ₂ ·H ₂ O]	1,1'-Bi-2-naphthol, mandelic acid, atenolol, 1,2-diphenylethylene glycol, 1,2-diphenylethanone, 3,5-dinitro-N-(1-phenylethyl) benzamide, DNB-leucine, chlorphenamine maleate, and ibuprofen	n-Hexane/isopropanol (99/1)	Packing (25 cm long × 4.6 mm i.d.)	0.69%	[138]
[Cu ₂ (D-Cam) ₂ (4,4'-bpy)] _n @SiO ₂	1-(9-Anthryl)-2,2,2-trifluoroethanol, salbutamol, 1-phenylethanol, 1-(4-chlorophenyl)ethanol, 3-benzyloxy-1,2-propanediol, alprenolol, praziquantel, flavanone, zopiclone, benzoic acid, furoin, trans-stilbene oxide, and Tröger's base	Different ratios of hexane/isopropanol with (v/v)	Packing (25 cm long × 2.1 mm i.d.)	1.0, 1.5, 3.0, and 2.0%	[139]
Homochiral MOF [Ni(S-mal)(bpy)] _n	Amlodipine, ibuprofen, flurbiprofen, propranolol, maleate chlorphenamine maleate and 1-p-chlorophenyl-ethanol	n-Hexane-isopropanol (8/2, 9/1, 95/5, 99/1)	Packing (25 cm long × 2.1 mm i.d.)	-	[140]
ZIF-8-PEI-CA	Tröger's base	MeOH/2-propanol (10/1)	Packing (6 cm length × 4.6 mm i.d.)	-	[141]
Chiral ionic liquid@MOF	Atenolol, propranolol, metoprolol, racecadotril, and raceanisodamine	MeOH/water (20/80)	Packing (25 cm length × 4.6 mm i.d.)	5%	[142]
TAMOF-1 (triazole acid MOF)	(±)-Ibuprofen and (±)-thalidomide	Acetonitrile	Packing (100 mm × 4.6 mm i.d.)	-	[114]

Table 2. Cont.

Type of MOF	Analyte	Mobile Phase	Form	Repeatability (RSD%)	Ref.
CMOF D-His-ZIF-L (DHZL)	S-1,1'-Bi-2-naphthol (S-BINOL)	n-Hexane/isopropanol (55/45)	Packing (25 cm length × 4.6 mm i.d.)	-	[143]
Magnetic graphene oxide- MOF [Zn ₂ (d-Cam) ₂ (4,4'-bpy)] _n (MGO-ZnCB)	1, 1'-Bi-2-naphthol (BN) and 2, 2'-furoin (Furoin)	Hexane/isopropanol (55/45)	Packing (25 cm length × 4.6 mm i.d.)	-	[144]
L-His-ZIF-8/Torlon®	1-Phenylethanol	0.1% Trifluoro acetic acid in n-hexane/EtOH (95/5)	Packing (25 cm length × 4.6 mm i.d.)	-	[145]

6.2. Gas Chromatography Enantioseparation

The use of GC enantiomer resolution with chiral MOFs is relatively new, and few studies currently exist. However, this is a beneficial method for separating molecules that can simply vaporize without decomposition [37]. In general, chiral capillary GC provides several advantages, including excellent resolution, sensitivity, efficiency, and the lack of liquid mobile phases. In practice, chiral capillary GC is mostly utilized to examine volatile and thermally stable racemic mixtures. Furthermore, because chiral capillary GC may be linked with mass spectrometry (MS) and solid-phase microextraction (SPME), it is an optimal method for the enantioseparation of enantiomers in complicated real samples. MOFs as stationary phases in GC show outstanding performance. The direct utilization of most of the “as-synthesized” MOFs, powders with heterogeneous particle sizes, in packed column GC as stationary-phase materials leads to displeasing gas resistance. The tight packing of tiny, irregularly sized particles of MOF results in a significant pressure decrease, especially in particles with a wide range of particle sizes. MOF-thin-coated capillary columns as a solution can help enhance separation efficiency [115,146]. MOFs as stationary phases in GC show outstanding performance. MOF-coated GC columns lead to a reduction in cost because of their low consumption for GC separation. Gas chromatographic separation is a simple and accessible platform for evaluating the interactions of MOF stationary phases with analytes compared to HPLC, because no liquid mobile phases in GC omit the interactions from solvents [147].

In recent years, different CMOFs have been employed in GC for enantiomer resolution because of their high thermal and chemical stability and great chiral framework structure. The standard processes of enantioseparation by GC possess four sections: (i) coating the internal GC column wall with CMOFs; (ii) applying a noble gas (e.g., helium (He), neon (Ne), argon (Ar), krypton (Kr), xenon (Xe), etc.) for the vaporization and infusion of racemates; (iii) the flow of racemates in the CMOF-coated column and their interaction with a CMOF for effective enantiomer resolution; and (iv) signal identification by a computer terminal [37]. Yuan and colleagues have made numerous contributions to this field. By applying the dynamic coating method, they coated four varieties of 3D-helical CMOFs, such as [(CH₃)₂NH₂][Cd(bpdc)_{1.5}·2DMA], MOF [Cd(LTP)₂]_n, Co(D-Cam)_{1/2}(bdc)_{1/2}(tmdpy), and Ni(D-cam)(H₂O)₂, on fused silica columns with success [148–151]. In brief, there was an introduction step of an ethanol suspension of each MOF into the column under gas pressure. After this, a wet coating layer on the inner wall of the column was obtained by pushing it through the column. As a restrictor, a long buffer tube was connected to the end of the capillary column to prevent the expedited solution from plugging near the column end. Last, nitrogen was used for flushing the MOF-coated fused silica column. These CMOFs exhibited great performance in the enantiomer resolution of a broad spectrum of racemates, such as camphor, citronellal, alanine, isoleucine, leucine, 2-methyl-1-butanol, 1-phenyl-1,2-ethanediol, phenylsuccinic acid isopropyl ester, proline trifluoroacetyl isopropyl ester derivatives, and 1-phenylethanol trifluoroacetyl derivatives, which mostly showed baseline separation. It is worth noting that the outcomes of some chromatographic separations were much better than those obtained with the commercial Chirasil-L-Val column. This strongly indicated the potential of CMOFs in racemate separation by GC.

In another study by Yuan and co-workers, a porous CMOF $\text{InH}(\text{D-C}_{10}\text{H}_{14}\text{O}_4)_2$ ($\text{D-C}_{10}\text{H}_{14}\text{O}_4 = \text{D-(+)-camphoric acid (D-H}_2\text{Cam)}$) was developed to coat the open tubular (OT) GC column for the enantioselective separation of racemates with high resolution because of its large surface area, great thermal stability, and remarkable chiral attributes [152]. $\text{InH}(\text{D-C}_{10}\text{H}_{14}\text{O}_4)_2$ has a left-handed helical channel with an anion-typed diamond network. The dynamic coating approach was used for coating OT columns with various lengths or inner diameters by $\text{InH}(\text{D-C}_{10}\text{H}_{14}\text{O}_4)_2$ for the gas chromatographic separation of various organic substances, such as alcohols, alkanes, isomers, and Grob's test compound. The separation factors (α) of citronellal, 1-phenyl-1,2-ethandiol, 1-phenyl-ethanol, 2-amino-1-butanol, limonene, methionine, and proline with the $\text{InH}(\text{D-C}_{10}\text{H}_{14}\text{O}_4)_2$ CSP were in the range of 1.10 to 1.44. A comparison between the chiral recognition capability of $\text{InH}(\text{D-C}_{10}\text{H}_{14}\text{O}_4)_2$ and the Chirasil-L-Val CSP indicated that proline and methionine had higher separation factors on prepared $\text{InH}(\text{D-C}_{10}\text{H}_{14}\text{O}_4)_2$ than on the Chirasil-L-Val CSP. Limonene and 1-phenylethanol did not show any separation on the Chirasil-L-Val CSP, whereas the $\text{InH}(\text{D-C}_{10}\text{H}_{14}\text{O}_4)_2$ CSP had good separation. All chiral separations on the developed CSP had short retention times of about 1.5 min and baseline separation for 2-amino-1-butanol, 1-phenylethanol, and 1-phenyl-1,2-ethandiol. The results revealed that the developed CSP possesses high selectivity and great recognition potential for these organic materials, especially for chiral substances. Moreover, Yuan et al. also reported the application of $\text{Zn}(\text{ISN})_2 \cdot 2\text{H}_2\text{O}$ with a huge left-handed channel ($\sim 8.6 \text{ \AA}$), a simple CMOF as a CSP for high-resolution gas chromatographic enantioseparation [153]. The dynamic coating strategy was employed for coating a fused-silica capillary column with $\text{Zn}(\text{ISN})_2 \cdot 2\text{H}_2\text{O}$. Then, the $\text{Zn}(\text{ISN})_2 \cdot 2\text{H}_2\text{O}$ -coated capillary column was applied for the enantiomer resolution of racemates (such as 1-phenyl-1,2-ethanediol, 1-phenylethanol, phenyl-succinic acid, citronellal, proline, and alanine), positional isomers, alcohols, and alkanes. The RSDs for five repeated alanine separations were 2.6% and 0.32% for peak area and retention time, respectively. The separation factors (α) of citronellal, phenyl-succinic acid, alanine, 1-phenyl-1,2-ethanediol, 1-phenylethanol, and proline with the $\text{Zn}(\text{ISN})_2 \cdot 2\text{H}_2\text{O}$ CSP were in the range of 1.18 to 1.46. The chiral separation ability of the $\text{Zn}(\text{ISN})_2 \cdot 2\text{H}_2\text{O}$ CSP was better than the Chirasil-L-Val CSP due to a higher separation factor of proline and alanine and great separation of 1-phenylethanol in the $\text{Zn}(\text{ISN})_2 \cdot 2\text{H}_2\text{O}$ -modified column. All analytes, except phenyl-succinic acid, had baseline separation. The developed novel chiral stationary phase demonstrated excellent selectivity, reproducibility, excessive column efficiency, and excellent chiral separation potential based on the obtained results.

In another study, Yuan and co-workers combined the excellent characteristics of CMOF $\text{InH}(\text{D-C}_{10}\text{H}_{14}\text{O}_4)_2$ with the novel features of peramylated β -CD to make a unique CSP for improved gas chromatographic enantioseparation [154]. Three capillary GC columns, including $\text{InH}(\text{D-C}_{10}\text{H}_{14}\text{O}_4)_2$, peramylated β -CD, and combined $\text{InH}(\text{D-C}_{10}\text{H}_{14}\text{O}_4)_2$ with peramylated β -CD, were employed for evaluating their racemate separation potentials. Seven racemates, including citronellal, dihydrocarvyl acetate, limonene, methyl L- β -hydroxyisobutyrate, menthol, DL-leucine, and 1-phenylethanol, were used for enantioseparation with the prepared columns. All the racemates had poor separation in column $\text{InH}(\text{D-C}_{10}\text{H}_{14}\text{O}_4)_2$, which showed the displayed separation of only three enantiomers. The second column contained peramylated β -CD and NaCl and separated five racemates, while the third column with $\text{InH}(\text{D-C}_{10}\text{H}_{14}\text{O}_4)_2$ and peramylated β -CD separated all seven compounds. For instance, 1-phenylethanol did not separate in columns $\text{InH}(\text{D-C}_{10}\text{H}_{14}\text{O}_4)_2$ or peramylated β -CD but separated in column $\text{InH}(\text{D-C}_{10}\text{H}_{14}\text{O}_4)_2$ incorporated with peramylated β -CD. In addition, the $\text{InH}(\text{D-C}_{10}\text{H}_{14}\text{O}_4)_2$ incorporated with peramylated β -CD column provided higher resolution for the separations of DL-leucine and dihydrocarvyl acetate in comparison to the peramylated β -CD column. Moreover, citronellal separated columns $\text{InH}(\text{D-C}_{10}\text{H}_{14}\text{O}_4)_2$ and $\text{InH}(\text{D-C}_{10}\text{H}_{14}\text{O}_4)_2$ incorporated with peramylated β -CD but did not separate in the peramylated β -CD column. Therefore, applying $\text{InH}(\text{D-C}_{10}\text{H}_{14}\text{O}_4)_2$ in cooperation with peramylated β -CD as a unique mixed chiral stationary phase enhanced the GC chiral separation and increased column efficiency.

The chromatograms of column $\text{InH}(\text{D-C}_{10}\text{H}_{14}\text{O}_4)_2$ incorporated with peramylated β -CD demonstrated good peaks with a minimum of 50% valley separation. This suggested that $\text{InH}(\text{D-C}_{10}\text{H}_{14}\text{O}_4)_2$ with a left-handed helical structure and diamond network exhibited the capacity for increasing the enantioselectivity and chiral recognition capability of peramylated β -CD. The RSDs of the column-to-column and run-to-run for the $\text{InH}(\text{D-C}_{10}\text{H}_{14}\text{O}_4)_2$ incorporated with peramylated β -CD column were 2.50% and 0.50%, respectively, which proved the good reproducibility of the prepared column. Moreover, Yuan et al. also combined another one of their developed CMOFs, $\text{Co}(\text{D-Cam})_{1/2}(\text{bdc})_{1/2}(\text{tmdpy})$, with peramylated β -CD for the GC enantioseparation of 10 chiral compounds: (RS)-linalool, (RS)-2-hexanol, (RS)-menthol, (RS)-citronellal, (RS)-limonene, (RS)-rose oxide, DL-leucin, DL-valine, (RS)-methyl L- β -hydroxyisobutyrate, and (RS)-dihydrocarvyl acetate [155]. The separation factor of the $\text{Co}(\text{D-Cam})_{1/2}(\text{bdc})_{1/2}(\text{tmdpy})$ incorporated with peramylated β -CD column was between 1.00 and 1.10. The separation of all enantiomers was poor in column $\text{Co}(\text{D-Cam})_{1/2}(\text{bdc})_{1/2}(\text{tmdpy})$, except for the citronellal separation that had a higher separation factor (column $\text{Co}(\text{D-Cam})_{1/2}(\text{bdc})_{1/2}(\text{tmdpy})$ (1.11) > column $\text{Co}(\text{D-Cam})_{1/2}(\text{bdc})_{1/2}(\text{tmdpy})$ incorporated with peramylated β -CD (1.08) > column peramylated β -CD (1.00). Columns $\text{Co}(\text{D-Cam})_{1/2}(\text{bdc})_{1/2}(\text{tmdpy})$ and peramylated β -CD had the ability of four and six racemates separation, respectively. The $\text{Co}(\text{D-Cam})_{1/2}(\text{bdc})_{1/2}(\text{tmdpy})$ incorporated with peramylated β -CD column separated nine enantiomers with good peaks, baseline or minimum of 60% valley separation, enhanced resolution, and good column efficacy. For repeatability, the RSDs of the CMOF-combined peramylated β -CD column were obtained from five successive linalool separations of 2.2% and 0.31% for the peak area and retention time, respectively. Additionally, the RSD for the column-column reproducibility was 6.2%. Based on these results, the developed method was reproducible and reliable. Thus, the use of $\text{Co}(\text{D-Cam})_{1/2}(\text{bdc})_{1/2}(\text{tmdpy})$ served an important role in the increased separation of chiral compounds. The intrinsic properties of $\text{Co}(\text{D-Cam})_{1/2}(\text{bdc})_{1/2}(\text{tmdpy})$, including a 3D-chiral network, perfect helicity, remarkable integration of molecular chirality, and high surface area, enable the cooperation of $\text{Co}(\text{D-Cam})_{1/2}(\text{bdc})_{1/2}(\text{tmdpy})$ with peramylated β -cyclodextrin to fabricate an attractive column for improved GC racemate separation.

Finally, in 2018, Yan et al. developed a PSM strategy for synthesizing CMOFs with various chiral sites for racemate resolution [156]. The parent MOF, MOF (MIL-101(Al)-NH₂), was employed due to its highly active amino groups and great structure. Then, based on the PSM of MIL-101(Al)-NH₂ and immobilization of various chiral ligands to the identical parent MOF, five different CMOFs were designed (Figure 17). The synthesized CMOFs were used for the fabrication of capillary columns for enantiomer resolution and analysis of several kinds of racemates with various chiral recognition sites. The CMOF-coated capillary GC columns showed superior enantioselective separation capability for different racemates compared to the commercial Cyclosil B and β -dex 225 chiral capillary columns. The CMOF-coated column showed good reproducibility for the chiral separation of citronellal with RSDs of 4.4%, 5.1%, and 0.2% for the peak area, peak height, and retention time, respectively. The RSDs of column-to-column and day-to-day for the citronellal separation CMOF-coated column were 5.0–7.1% and 2.0–2.6%, respectively. The results indicated that the PSM method is helpful for creating pre-designed functional CMOFs, as novel CSPs provide a broad spectrum of chromatographic racemates separation.

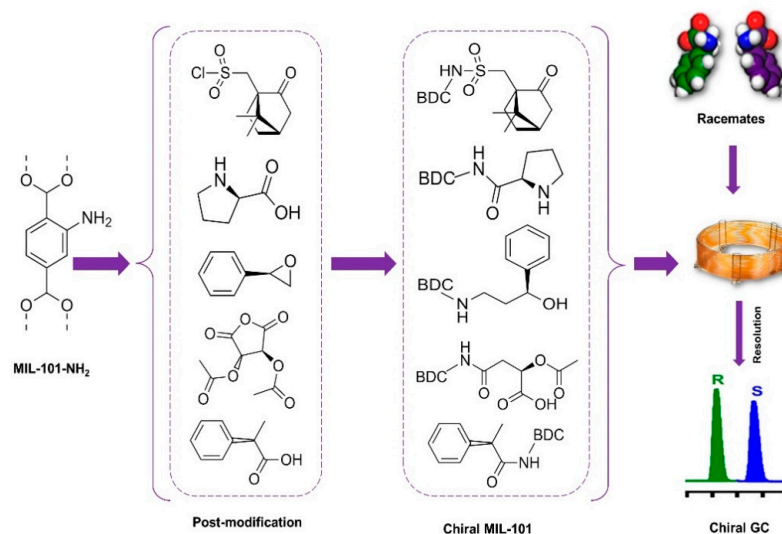


Figure 17. Scheme of the post-modification of chiral MIL-101(AI)-Xs and the construction of chiral GC by coated capillary columns [156]. Redraw by PowerPoint 365 software.

6.3. Capillary Electrochromatography Racemate Resolution

Capillary electrophoresis (CE) has various separation modes offering multiple options for separating analytes. In CEC, a stationary phase is applied to enhance separation performance. CEC is an analytical method combining the excellent separation efficacy of CE with the selectivity provided by LC [157]. The application of MOFs as CSPs in CEC has been confirmed to be useful for racemate resolution analysis. However, an efficient strategy is deficient for capillary column modification with MOFs. Mainly, MOF-based capillary columns are classified into three types: packed columns, OT columns, or monolithic columns.

In 2014, Yuan and co-workers employed a homochiral-helical MOF $[\text{Zn}_2(\text{D}(+)\text{-camphoric acid})_2(4,4'\text{-bipyridine})]_n$ as a CSP in OT-CEC (a homochiral MOF-coated OT-CEC) for the resolution of positional isomers (e.g., nitrophenol and ionone) and two chiral compounds, flavanone and praziquantel [158]. The reported homochiral-helical MOF was composed of homochiral layers with pillars of bipyridine ligands for creating two kinds of 3D six-connected self-permeable structures. The inner wall of the OT-column was pretreated with a sodium silicate solution to have a stable layer of stationary phase, which was an MOFs' post-coated process for the fabrication of the $[\text{Zn}_2(\text{D}(+)\text{-camphoric acid})_2(4,4'\text{-bipyridine})]_n$ -coated OT column. The baseline separation of praziquantel and flavanone with $[\text{Zn}_2(\text{D}(+)\text{-camphoric acid})_2(4,4'\text{-bipyridine})]_n$ -coated OT-CEC showed great column efficacy and enhanced resolution. Different chromatographic parameters, including pH, the concentration of buffer, and the addition of organic modifiers, were evaluated to achieve the best separation. The RSDs for the column-to-column, day-to-day, and retention time of run-to-run were 3.07%, 2.16%, and 1.04%, respectively. The results showed that CMOFs are useful for enantiomer resolution in CEC.

In 2016, Zong et al. synthesized a homochiral MOF $[\text{Zn}_2(\text{D-Cam})_2(4,4'\text{-bpy})]_n$ with a large particle size covalently linked to the capillary inner walls [159]. The $[\text{Zn}_2(\text{D-Cam})_2(4,4'\text{-bpy})]_n$ -modified capillary column showed successful enantioseparation performance for DL-Tyr and DL-Phe. The MOF $[\text{Zn}_2(\text{D-Cam})_2(4,4'\text{-bpy})]_n$ -coated capillary column demonstrated a broad linear range and excellent thermal stability. The intraday, interday, and column-to-column stability of the MOF-coated capillary column for DL-Phe and DL-Tyr were 0.57–12.13% and 0.45–9.93%, respectively. A recent study by Chen and colleagues used a pepsin-ZIF-8-modified poly(GMA-co-EDMA) monolithic column [160]. Poly(glycidyl methacrylate)-co-ethylene dimethacrylate monoliths were employed as support for the growth of MOF ZIF-8 (zeolitic imidazolate framework-8) through layer-by-layer self-assembly (Figure 18). The Schiff base method was employed for the

covalent linkage of pepsin, which served as a chiral selector on the amino-functionalized ZIF-8 surface. The amino groups for the functionalization of ZIF-8 were provided by N-(3-aminopropyl)imidazole. Zeolitic imidazolate framework-8 supplied stable conditions for enantioseparation and improved the chiral resolution. The pepsin-ZIF8-poly(GMA-co-EDMA) column showed the capability for the enantiomer separation of six racemic drugs, chloroquine, nefopam, hydroxychloroquine, clenbuterol, amlodipine, and hydroxyzine, within 15 min. The pepsin-ZIF8-poly(GMA-co-EDMA) column demonstrated great improvement of resolution compared to the pepsin-poly(GMA-co-EDMA) column (without ZIF-8). Compared to the pepsin-poly(GMA-co-EDMA) column (without ZIF-8), there was considerable resolution enhancement (hydroxychloroquine: 0.34 → 2.50; chloroquine: 0.45 → 1.97; hydroxyzine: 0.39 → 1.43; nefopam: 0.27 → 0.81; clenbuterol: 0 → 0.81; amlodipine: 0.16 → 0.72). The day-to-day and run-to-run reproducibility of RSDs and Rs were both <4.50%. Five batches of pepsin-ZIF-8@GMA columns with the same procedure were run to evaluate column-to-column reproducibility. The RSDs values of Rs and the retention time of four columns were less than 7.63% and 7.12%. These results exhibit the good reproducibility of the pepsin-ZIF-8@GMA columns.

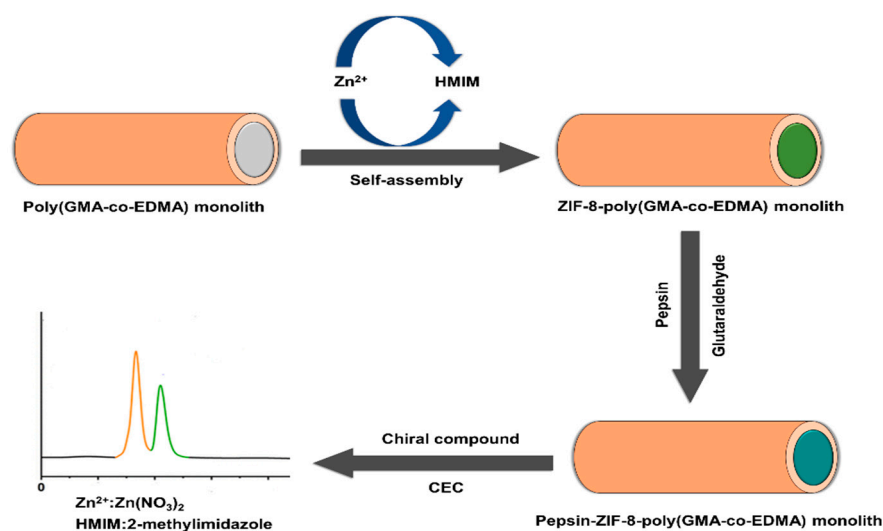


Figure 18. Illustration of the fabrication steps of pepsin-ZIF-8@GMA monolithic column for CEC racemate resolution [160]. Redraw by PowerPoint 365 software.

In 2021, Chen et al. developed a homochiral MOF L-His-NH-MIL-53-based capillary column for racemate separation by CEC [161]. Achiral nanocrystalline MIL-53 was synthesized through a PSM procedure, and it resulted in the fabrication of a homochiral MOF termed L-His-NH-MIL-53. L-His-NH-MIL-53 was used as a chiral coating of OT-CEC for the enantioselective separation of D-/L-Trp; D-/L-Phe; and four basic drugs: metoprolol, amlodipine, esmolol, and bisoprolol. The porous structure of the fabricated homochiral MOF L-His-NH-MIL-53 served as a crucial feature in advancing the enantioselectivity of L-His because it can render adequate sites for interactions of L-His with enantiomers. This research not only employed a new homochiral MOF for the coating of the OT-capillary column but also demonstrated that the enantioselectivity of L-His as a weak chiral recognition reagent can be considerably improved through integration with MOFs. In 2022, Bingbing et al. synthesized a novel type of chiral zirconium-based homogeneous CMOF, L-Cys-PCN-222, in which PCN-222 and L-Cys were employed as a framework and chiral modifier, respectively, through the solvent-assisted ligand incorporation approach [162]. L-Cys-PCN-222 was used as the CSP through bonding to the inner wall of the OT-column in CEC for the enantioseparation of amino acids (such as serine, methionine, threonine, Asp, Lys, glutamic acid, His, and arginine); herbicide pesticides (like imazameth, imazethapyr, imazamox, quizalofop-p-ethyl, and diclofop); and fluoroquinolone drugs, including lomefloxacin hydrochloride, ofloxacin, flumequine, and gatifloxacin. Based on

the results, L-Cys-PCN-222 showed advantages, including thermal stability, high specific surface area, good crystallinity, and chiral separation performance. The separation factor (α) and degree of separation (R_s) of the analytes differed in the ranges of 1.07 to 3.27 and 0.61 to 26.0, respectively. The maximum degree of separation (26.0) pointed to the outstanding enantioseparation performance of the L-Cys-PCN-222-bonded OT column. The RSDs of the column efficiencies for runs, column-to-column, day-to-day, and run-to-run were 2.73%, 6.62%, 2.37%, and 1.39%, respectively. In addition, there was no obvious alteration after 200 runs. The results demonstrated higher column efficacy and prolonged lifetime of the innovative zirconium-based stationary phase for enantiomer resolution.

Du and colleagues synthesized a homochiral Fe-CD-MOF (iron-based γ -CD MOF) with mesoporous as a CSP of OT-CEC for the enantioseparation of 1 chiral alcohol and 14 racemic drugs, including anisodamine, ephedrine, pseudoephedrine, ritodrine, promethazine, sotalol, galantamine, laudance, synephrine, quinine/quinidine, oxybutynin, cinchonine/cinchonidine, (RS)-pseudotropine, nefopam, terbutaline, and octopamine [163]. The 3D-cubic homochiral Fe-CD-MOF was covalently attached to the isocyanate propyl triethoxy silane (IPTS)-modified capillary inner wall (Fe-CD-MOF@IPTS-coated capillary column). For the first time, γ -cyclodextrin-based MOF containing Fe (III) ions were employed for stereoisomer separation. The designed Fe-CD-MOF@IPTS-coated OT-column demonstrated excellent stability and repeatability with RSDs of <1.7%, <3.5%, and <6.5% for run-to-run, day-to-day, and column-to-column, respectively. The Fe-CD-MOF@IPTS-modified column showed great separation performance for chiral alcohol and 14 racemic drugs. The best R_s of anisodamine, ephedrine/pseudoephedrine, and ritodrine were 17.07, 6.93, and 7.65. The retention time was less than seven minutes, demonstrating the high efficiency of the Fe-CD-MOF@IPTS-modified column. Furthermore, the enantiomer resolution mechanism of the homochiral Fe-CD-MOF-coated column was studied using adsorption kinetic experiments. According to the results, renewable and homochiral Fe-CD-MOF showed outstanding potential in the chiral stationary-phase racemate separation with CEC. Another study by Du et al. showed a water-stable achiral zeolite-imidazole MOF-like metal salt (4, 5-IMD-Zn) in cooperation with a natural chiral selector carboxymethyl (CM)- β -CD, creating a great synergistic system for OT-CEC [164]. For preparing the coated columns, the growth of MOF NPs was provoked on the inner wall of the imidazolyl functional column. The synergistic separation system resulted in the baseline resolutions of atenolol, ofloxacin, and hydroxychloroquine. Based on the results, the separation resolution of three basic drugs improved compared to the bare capillary. The RSDs were 2.1, 2.6, and 5.2% for the run-to-run, day-to-day, and column-to-column retention time, respectively. The stability of the 4, 5-IMD-Zn-modified OT-column was evaluated by keeping the prepared column at 4 °C for more than four months and then employed to test the R_s of atenolol. Compared to the data from four months ago, the RSD of the R_s was <5.1%, demonstrating the good stability of the prepared column up to four months at 4 °C. This study expanded achiral MOFs performance in CEC for enantiomer resolution and supplied an affordable synergistic separation system for commercial application.

Du and co-workers also designed a novel capillary monolith column with a combination of properties of MOF-5 and pepsin as a chiral selector for racemate resolution [165]. The layer-by-layer self-assembly approach was employed for inducing the growth of MOF-5 on the original monolith of poly(GMA-co-EDMA) (poly (glycidyl methacrylate-co-ethylene dimethacrylate)). Then, pepsin was covalently attached to the MOF-5 carboxyl group by an amidation reaction under the catalysis of N-(3-dimethylaminopropyl)-N'-ethylcarbodiimide and N-hydroxysuccinimide (Figure 19). Ultimately, the developed pepsin@MOF-5@poly(GMA-co-EDMA) column was employed for the enantiomer separation of six basic racemic drugs: chloroquine, hydroxychloroquine, clenbuterol, nefopam, hydroxyzine, and chlorpheniramine. The RSDs of R_s and migration time for interday and intraday were <4.0%, whereas the RSDs of column-to-column were <6.6%, demonstrating the good repeatability of the developed column. The pepsin-MOF-5-modified column obtained great chromatographic resolutions ($R_s = 1.74$ and 2.41) for chloroquine

and hydroxychloroquine under optimal conditions, respectively. Moreover, the prepared column showed rapid enantioseparation within 15 min. This reveals that the modification of capillary monolithic columns with MOFs causes good racemates separation by CEC.

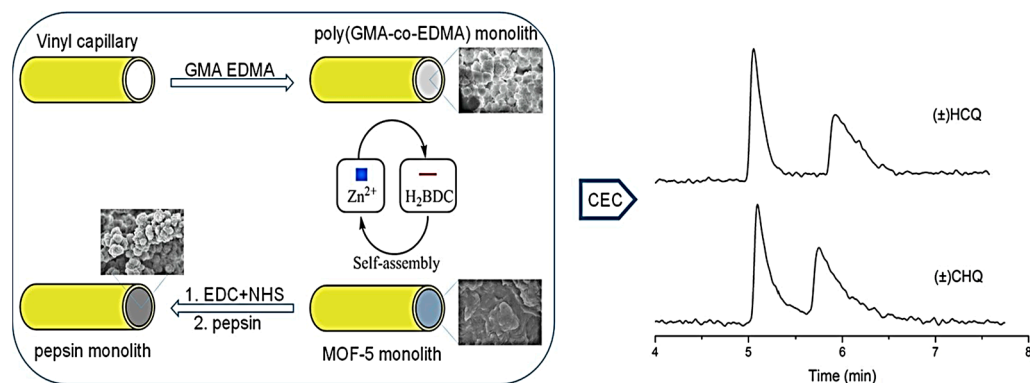


Figure 19. A layer-by-layer self-assembly of MOF-5 and pepsin as a chiral selector to prepare new monolithic capillary columns. Because of the synergistic effect of MOF and pepsin, the developed capillary column could complete the racemate resolution of 6 chiral drugs within 15 min with good repeatability and stability. Layered MOF-5 is the key to enhancing the performance of capillary columns, and its application in CEC is also one of the advanced trends in the future. Reprinted (adapted) with permission from [165].

Wang and colleagues fabricated a new chiral stationary phase of a zirconium (Zr)-based MOF named L-Cys-PCN-224 using the one-pot procedure for enantiomer resolution by CEC [166]. The L-Cys-PCN-224 was attached to the OT-column and used for the enantiomer separation of nine types of natural amino acids, including neutral leucine, glutamine, methionine, Trp, proline, phenylalanine, valine, basic His, and acidic Asp (Figure 20). Based on the achieved results, the prepared chiral stationary phase possessed a high specific surface area, excellent crystallinity, and thermal stability. Meanwhile, the scanning electron microscope confirmed the successful linkage of the L-Cys-PCN-224 to the inner walls of the OT column. The RSDs for the average column efficiency and the migration time of column-to-column, day-to-day, and run-to-run were 0.62–9.14%. The lifetime of the L-Cys-PCN-224-modified column was evaluated by the RSDs of migration time, and the column efficiency for 200 successive injections was <4.38% and <7.81%, respectively. According to the obtained results, the L-Cys-PCN-224-linked OT column demonstrated a longer lifetime, good reproducibility, and stability. Chiral resolution performance was proved for the neutral, acidic, and basic amino acids with a resolution of 1.38–13.9. These results demonstrated that the CSP had excellent potential in the chiral separation field. The results show the essential roles of hydrogen bonding, steric fit, electrostatic interaction, and π - π interaction between the analytes and the CSP crystal structure. Table 3 provides a summary of CMOFs as CSPs for CEC.

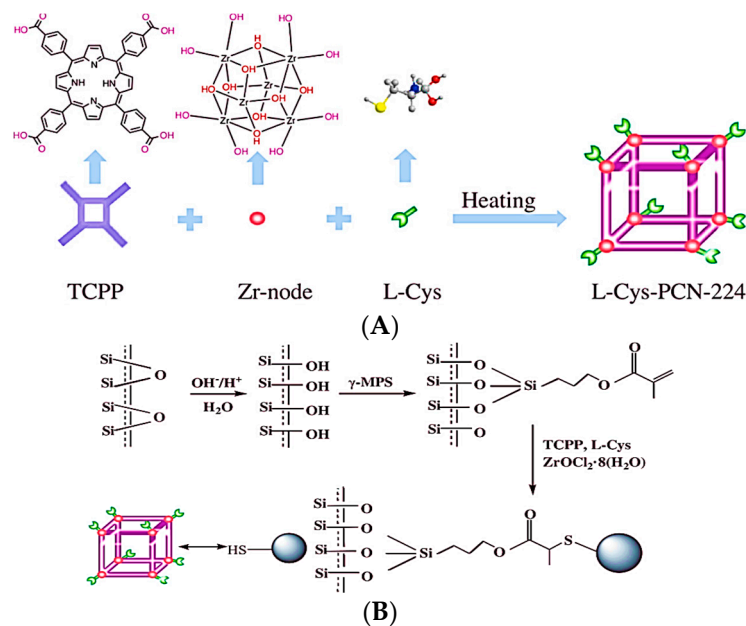


Figure 20. (A) Scheme of the L-Cys-PCN-224 synthesis process. (B) Fabrication of L-Cys-PCN-224-bonded OT-column. Reprinted (adapted) with permission from [166].

Table 3. Chiral MOFs as chiral stationary phases for CEC.

Separation Mode	Type of MOF	Chiral Selector	Analyte	Column Preparation Strategy	RSD% (Run-to-Run, Day-to-Day, and Column-to-Column)	Ref.
Packed CEC	$[\text{In}_3\text{O}(\text{obb})_3(\text{HCO}_2)(\text{H}_2\text{O})] \cdot \text{solvents}$	-	(\pm)-hydrobenzoin, (\pm)-1-phenyl-1,2-ethanediol, and clenbuterol	Pressurized packing	1.51–3.63, 1.83–3.98, and 3.42–5.66%	[167]
OT-CEC	HKUST-1 of type $\text{Cu}_3(\text{BTC})_2$ (or MOF-199)	carboxymethyl- β -cyclodextrin	propranolol, esmolol, metoprolol, amlodipine and sotalol		5.00, 6.60, and 7.5%	[168]
OT-CEC	zeolite-like MOF JLU-Liu23	-	epinephrine, isoprenaline, and synephrine and their analog terbutaline	Dynamic coating	0.3–0.6%, 0.8–2.2% and 3.5–6.5%	[169]
OT-CEC	ZIF-90	lactobionic acid	propranolol, metoprolol, atenolol, bisoprolol, and sotalol	In situ synthesis	1.8, 2.7, and 7.4%	[170]
OT-CEC	$[\text{Cu}(\text{mal})(\text{bpy})] \cdot \text{H}_2\text{O}$	-	ephedrine, pseudoephedrine, penicillamine, L-penicillamine, D-phenylalanine, L-phenylalanine	Covalent bonding	0.38–0.41, 0.41–0.42, and 2.22–2.65%	[171]
OT-CEC	AlaZnCl	-	isoprenaline, synephrine, norepinephrine, epinephrine, terbutaline, and carvedilol	In situ synthesis	0.56–0.55, 1.20–0.93, 4.01–3.81%	[172]
OT-CEC	PDA- γ -CD-MOF(Cu-SD)	γ -cyclodextrin	dansyl (Dns)-DL-phenylalanine, Dns-DL-leucine, Dns-DL-valine, Dns-DL-threonine, and Dns-DL-serine	Static coating	0.27, 1.45 and 4.88%	[173]
OT-CEC	BSA@ZIF-8	-	methylparaben, ethylparaben, propylparaben, butylparaben, position isomers, Ephedrine and pseudoephedrine	Dynamic coating	4.1–5.3, 5.5–6.7, and 7.4–8.7%	[174]

7. Conclusions and Future Perspectives

This thoroughly summarized review discussed MOFs and their applications, especially in chiral analysis. Although the research application of MOFs is only from the last two decades, no comprehensive review has been presented on MOFs in the sub-branches of

chiral recognition and separation techniques. MOFs are emerging as the latest class of crystalline nanoporous materials and a very efficient substance for diverse chiral recognition and separation applications. The high modularity, inherent chirality, and simplicity of CMOFs' functionalization allow the improvement of many unique chiral materials for advanced applications. In comparison to conventional chiral solid substances, including chiral carbons, chiral zeolites, and chiral amorphous polymers, CMOFs are prominent and outstanding because of their capacity for the perfect combination of tunability, excessive enantiopurity, single crystallinity, excellent designability, and limitless pore/structural diversity. These characteristics enable the superb tuning of material features and the accurate knowledge of relationships between property and structure at the molecular level. We compressively summarized chirality, the principles of chiral analysis, and the state-of-the-art accomplishments of MOFs in an extensive scope of enantioselective performances, with the primary space allotted to chiral recognition and separation.

The growing demand for enantiopure composites has provoked rapid progress in applying functional materials for enantioseparation strategies. Using chromatographic methods, natural and synthetic polymers have long had the capacity for enantioselective resolution by roughly 90%. Even though chiral polymer-based racemic resolutions have made outstanding accomplishments, there are still difficulties regarding the separation mechanism. Considering this, CMOFs with manageable chiral cavities and specific crystalline configurations are the most appropriate candidates for preparative and analytical separations of racemates. It is hoped that a thorough examination of the racemic separation mechanism at the molecular level would remarkably expedite and extend CMOF-based enantioseparation.

In modern chemical analysis, the enantioselective sensing field has emerged because of the highest level of chirality complexity, and enantiospecific determination between racemic materials is incorporated in approximately every chiral process. Subsequently, the enantiorecognition of racemic molecules through the application of suitable analytical approaches, including fluorescence, electrochemical, QCM, and CD methods, has received substantial attention from researchers. It seems that CMOFs are intrinsically sensitive to chiral guests because of their concentration capacity of various targets at higher levels. However, the virtuous potential of CMOFs as enantioselective sensors has not completely manifested due to insufficient principles of design as well as inadequate chiral systems.

Nevertheless, integrating MOFs with chiral recognition and separation technologies is progressively assumed to be a promising avenue toward high-performance enantioselective determination and separations. In the following decades, it is optimistic that CMOFs will become one of the pivotal substances in chirotechnology. In this respect, close cooperation between engineers and scientists from various disciplines is exceedingly needed to solve challenges and evaluate the actual performance of MOFs in related areas.

Author Contributions: Writing—original draft preparation, S.H. and N.N.; writing—review and editing, J.P. All authors have read and agreed to the published version of the manuscript.

Funding: The support from the project DSGC-2021-0176 was founded under the OPIE project "Improvement of Doctoral Student Grant Competition Schemes and their Pilot Implementation" reg. no. CZ.02.2.69/0.0/0.0/19_073/0016713 is gratefully acknowledged.

Institutional Review Board Statement: Not applicable.

Informed Consent Statement: Not applicable.

Data Availability Statement: Not applicable.

Conflicts of Interest: The authors declare no conflict of interest.

References

1. Milton, F.P.; Govan, J.; Mukhina, M.V.; Gun'ko, Y.K. The chiral nano-world: Chiroptically active quantum nanostructures. *Nanoscale Horiz.* **2016**, *1*, 14–26. [[CrossRef](#)] [[PubMed](#)]
2. Stalcup, A.M. Chiral separations. *Annu. Rev. Anal. Chem.* **2010**, *3*, 341–363. [[CrossRef](#)] [[PubMed](#)]
3. Andrushko, V.; Andrushko, N. Principles, concepts, and strategies of stereoselective synthesis. *Stereoselective Synth. Drugs Nat. Prod.* **2013**, 3–44. [[CrossRef](#)]
4. Purcell-Milton, F.; McKenna, R.; Brennan, L.J.; Cullen, C.P.; Guillemeney, L.; Tepliakov, N.V.; Baimuratov, A.S.; Rukhlenko, I.D.; Perova, T.S.; Duesberg, G.S. Induction of chirality in two-dimensional nanomaterials: Chiral 2D MoS₂ nanostructures. *ACS Nano* **2018**, *12*, 954–964. [[CrossRef](#)] [[PubMed](#)]
5. Duerinck, T.; Denayer, J. Metal–organic frameworks as stationary phases for chiral chromatographic and membrane separations. *Chem. Eng. Sci.* **2015**, *124*, 179–187. [[CrossRef](#)]
6. Song, L.; Pan, M.; Zhao, R.; Deng, J.; Wu, Y. Recent advances, challenges and perspectives in enantioselective release. *J. Control. Release* **2020**, *324*, 156–171. [[CrossRef](#)]
7. Trojanowicz, M. Enantioselective electrochemical sensors and biosensors: A mini-review. *Electrochem. Commun.* **2014**, *38*, 47–52. [[CrossRef](#)]
8. D'Orazio, G.; Fanali, C.; Asensio-Ramos, M.; Fanali, S. Chiral separations in food analysis. *TrAC Trends Anal. Chem.* **2017**, *96*, 151–171. [[CrossRef](#)]
9. Rocco, A.; Aturki, Z.; Fanali, S. Chiral separations in food analysis. *TrAC Trends Anal. Chem.* **2013**, *52*, 206–225. [[CrossRef](#)]
10. Davankov, V.A. The nature of chiral recognition: Is it a three-point interaction? *Chirality* **1997**, *9*, 99–102. [[CrossRef](#)]
11. Chen, S.; Ward, T. Comparison of the chiral separation of amino-acid derivatives by a teicoplanin and RN- β -CD CSPs using waterless mobile phases: Factors that enhance resolution. *Chirality Pharmacol. Biol. Chem. Conseq. Mol. Asymmetry* **2004**, *16*, 318–330.
12. Nakano, Y.; Konya, Y.; Taniguchi, M.; Fukusaki, E. Development of a liquid chromatography-tandem mass spectrometry method for quantitative analysis of trace d-amino acids. *J. Biosci. Bioeng.* **2017**, *123*, 134–138. [[CrossRef](#)] [[PubMed](#)]
13. Zhou, X.; Zuo, C.; Li, W.; Shi, W.; Zhou, X.; Wang, H.; Chen, S.; Du, J.; Chen, G.; Zhai, W. A novel D-peptide identified by mirror-image phage display blocks TIGIT/PVR for cancer immunotherapy. *Angew. Chem. Int. Ed.* **2020**, *59*, 15114–15118. [[CrossRef](#)] [[PubMed](#)]
14. Fanali, S.; Chankvetadze, B. History, advancement, bottlenecks, and future of chiral capillary electrochromatography. *J. Chromatogr. A* **2021**, *1637*, 461832. [[CrossRef](#)] [[PubMed](#)]
15. Lin, Z.; Lv, S.; Zhang, K.; Tang, D. Optical transformation of a CdTe quantum dot-based paper sensor for a visual fluorescence immunoassay induced by dissolved silver ions. *J. Mater. Chem. B* **2017**, *5*, 826–833. [[CrossRef](#)] [[PubMed](#)]
16. Pätzold, R.; Brückner, H. Gas chromatographic determination and mechanism of formation of D-amino acids occurring in fermented and roasted cocoa beans, cocoa powder, chocolate and cocoa shell. *Amino Acids* **2006**, *31*, 63–72. [[CrossRef](#)]
17. West, C. Recent trends in chiral supercritical fluid chromatography. *TrAC Trends Anal. Chem.* **2019**, *120*, 115648. [[CrossRef](#)]
18. Huang, X.-Y.; Pei, D.; Liu, J.-F.; Di, D.-L. A review on chiral separation by counter-current chromatography: Development, applications and future outlook. *J. Chromatogr. A* **2018**, *1531*, 1–12. [[CrossRef](#)]
19. Liang, Y.-D.; Song, J.-F. Flow-injection chemiluminescence determination of tryptophan through its peroxidation and epoxidation by peroxy-nitrous acid. *J. Pharm. Biomed. Anal.* **2005**, *38*, 100–106. [[CrossRef](#)]
20. Vashistha, V.K.; Sethi, S.; Kumar, A.; Ahmed, S.; Das, D.K. Application of NMR Spectroscopy in Chiral Recognition of Drugs. *Appl. NMR Spectrosc.* **2021**, *9*, 131.
21. Han, D.-Q.; Yao, Z.-P. Chiral mass spectrometry: An overview. *TrAC Trends Anal. Chem.* **2020**, *123*, 115763. [[CrossRef](#)]
22. Gao, Z.; Liu, N.; Cao, Q.; Zhang, L.; Wang, S.; Yao, W.; Chao, F. Immunochip for the detection of five kinds of chemicals: Atrazine, nonylphenol, 17-beta estradiol, paraverine and chloramphenicol. *Biosens. Bioelectron.* **2009**, *24*, 1445–1450. [[CrossRef](#)] [[PubMed](#)]
23. Yuan, H.; Huang, Y.; Yang, J.; Guo, Y.; Zeng, X.; Zhou, S.; Cheng, J.; Zhang, Y. An aptamer-based fluorescence bio-sensor for chiral recognition of arginine enantiomers. *Spectrochim. Acta Part A Mol. Biomol. Spectrosc.* **2018**, *200*, 330–338. [[CrossRef](#)] [[PubMed](#)]
24. Zhang, Q.; Xue, S.; Li, A.; Ren, S. Functional materials in chiral capillary electrophoresis. *Coord. Chem. Rev.* **2021**, *445*, 214108. [[CrossRef](#)]
25. Rutkowska, M.; Płotka-Wasyłka, J.; Morrison, C.; Wieczorek, P.P.; Namieśnik, J.; Marć, M. Application of molecularly imprinted polymers in analytical chiral separations and analysis. *TrAC Trends Anal. Chem.* **2018**, *102*, 91–102. [[CrossRef](#)]
26. Wu, Q.; Lv, H.; Zhao, L. Applications of carbon nanomaterials in chiral separation. *TrAC Trends Anal. Chem.* **2020**, *129*, 115941. [[CrossRef](#)]
27. Tiwari, M.P.; Prasad, A. Molecularly imprinted polymer based enantioselective sensing devices: A review. *Anal. Chim. Acta* **2015**, *853*, 1–18. [[CrossRef](#)]
28. Fanali, C. Enantiomers separation by capillary electrochromatography. *TrAC Trends Anal. Chem.* **2019**, *120*, 115640. [[CrossRef](#)]
29. Zhang, Q. Ionic liquids in capillary electrophoresis for enantioseparation. *TrAC Trends Anal. Chem.* **2018**, *100*, 145–154. [[CrossRef](#)]
30. Furukawa, H.; Cordova, K.E.; O'Keeffe, M.; Yaghi, O.M. The chemistry and applications of metal-organic frameworks. *Science* **2013**, *341*, 1230444. [[CrossRef](#)]
31. Lei, J.; Qian, R.; Ling, P.; Cui, L.; Ju, H. Design and sensing applications of metal–organic framework composites. *TrAC Trends Anal. Chem.* **2014**, *58*, 71–78. [[CrossRef](#)]

32. Bhattacharjee, S.; Khan, M.I.; Li, X.; Zhu, Q.-L.; Wu, X.-T. Recent progress in asymmetric catalysis and chromatographic separation by chiral metal–organic frameworks. *Catalysts* **2018**, *8*, 120. [[CrossRef](#)]
33. Liu, K.-G.; Sharifzadeh, Z.; Rouhani, F.; Ghorbanloo, M.; Morsali, A. Metal-organic framework composites as green/sustainable catalysts. *Coord. Chem. Rev.* **2021**, *436*, 213827. [[CrossRef](#)]
34. Berthod, A. Chiral recognition mechanisms in enantiomers separations: A general view. In *Chiral Recognition in Separation Methods*; Springer: Berlin/Heidelberg, Germany, 2010; pp. 1–32.
35. Yan, Z.-H.; Li, D.; Yin, X.-B. Review for chiral-at-metal complexes and metal-organic framework enantiomorphs. *Sci. Bull.* **2017**, *62*, 1344–1354. [[CrossRef](#)]
36. Rocío-Bautista, P.; Taima-Mancera, I.; Pasán, J.; Pino, V. Metal-organic frameworks in green analytical chemistry. *Separations* **2019**, *6*, 33. [[CrossRef](#)]
37. Gong, W.; Chen, Z.; Dong, J.; Liu, Y.; Cui, Y. Chiral Metal–Organic Frameworks. *Chem. Rev.* **2022**, *122*, 9078–9144. [[CrossRef](#)]
38. Yuan, S.; Deng, Y.-K.; Xuan, W.-M.; Wang, X.-P.; Wang, S.-N.; Dou, J.-M.; Sun, D. Spontaneous chiral resolution of a 3D (3, 12)-connected MOF with an unprecedented ttt topology consisting of cubic [Cd 4 (μ 3-OH) 4] clusters and propeller-like ligands. *CrystEngComm* **2014**, *16*, 3829–3833. [[CrossRef](#)]
39. Sharifzadeh, Z.; Berijani, K.; Morsali, A. Chiral metal–organic frameworks based on asymmetric synthetic strategies and applications. *Coord. Chem. Rev.* **2021**, *445*, 214083. [[CrossRef](#)]
40. Berijani, K.; Chang, L.-M.; Gu, Z.-G. Chiral templated synthesis of homochiral metal-organic frameworks. *Coord. Chem. Rev.* **2023**, *474*, 214852. [[CrossRef](#)]
41. Yutkin, M.; Zavakhina, M.; Samsonenko, D.; Dybtsev, D.; Fedin, V. Porous homo- and heterochiral cobalt (II) aspartates with high thermal stability of the metal-organic framework. *Russ. Chem. Bull.* **2010**, *59*, 733–740. [[CrossRef](#)]
42. Burchell, T.J.; Puddephatt, R.J. Homochiral and heterochiral coordination polymers and networks of silver (I). *Inorg. Chem.* **2006**, *45*, 650–659. [[CrossRef](#)] [[PubMed](#)]
43. Zhang, M.; Dai, Q.; Zheng, H.; Chen, M.; Dai, L. Novel MOF-derived Co@N-C bifunctional catalysts for highly efficient Zn-air batteries and water splitting. *Adv. Mater.* **2018**, *30*, 1705431. [[CrossRef](#)] [[PubMed](#)]
44. Aerts, H.J.; Velazquez, E.R.; Leijenaar, R.T.; Parmar, C.; Grossmann, P.; Carvalho, S.; Bussink, J.; Monshouwer, R.; Haibe-Kains, B.; Rietveld, D.; et al. Corrigendum: Decoding tumour phenotype by noninvasive imaging using a quantitative radiomics approach. *Nat. Commun.* **2014**, *5*, 4644. [[CrossRef](#)]
45. Newsam, J.; Treacy, M.M.; Koetsier, W.; Gruyter, C.D. Structural characterization of zeolite beta. *Proc. R. Soc. London. A. Math. Phys. Sci.* **1988**, *420*, 375–405.
46. Peng, Y.; Gong, T.; Zhang, K.; Lin, X.; Liu, Y.; Jiang, J.; Cui, Y. Engineering chiral porous metal-organic frameworks for enantioselective adsorption and separation. *Nat. Commun.* **2014**, *5*, 4406. [[CrossRef](#)]
47. Wang, X.; Lamprou, A.; Svec, F.; Bai, Y.; Liu, H. Polymer-based monolithic column with incorporated chiral metal–organic framework for enantioseparation of methyl phenyl sulfoxide using nano-liquid chromatography. *J. Sep. Sci.* **2016**, *39*, 4544–4548. [[CrossRef](#)]
48. Zor, E.; Bingol, H.; Ersoz, M. Chiral sensors. *TrAC Trends Anal. Chem.* **2019**, *121*, 115662. [[CrossRef](#)]
49. Huang, H.; Bian, G.; Zong, H.; Wang, Y.; Yang, S.; Yue, H.; Song, L.; Fan, H. Chiral sensor for enantiodiscrimination of varied acids. *Org. Lett.* **2016**, *18*, 2524–2527. [[CrossRef](#)]
50. Niu, X.; Yang, X.; Li, H.; Liu, J.; Liu, Z.; Wang, K. Application of chiral materials in electrochemical sensors. *Microchim. Acta* **2020**, *187*, 676. [[CrossRef](#)]
51. Liu, D.; Lu, K.; Poon, C.; Lin, W. Metal–organic frameworks as sensory materials and imaging agents. *Inorg. Chem.* **2014**, *53*, 1916–1924. [[CrossRef](#)]
52. Saadati, A.; Hassanpour, S.; de la Guardia, M.; Mosafer, J.; Hashemzaei, M.; Mokhtarzadeh, A.; Baradaran, B. Recent advances on application of peptide nucleic acids as a bioreceptor in biosensors development. *TrAC Trends Anal. Chem.* **2019**, *114*, 56–68. [[CrossRef](#)]
53. Kholafazad Kordasht, H.; Hassanpour, S.; Baradaran, B.; Nosrati, R.; Hashemzaei, M.; Mokhtarzadeh, A.; de la Guardia, M. Biosensing of microcystins in water samples; recent advances. *Biosens. Bioelectron.* **2020**, *165*, 112403. [[CrossRef](#)] [[PubMed](#)]
54. Pugh, V.J.; Hu, Q.S.; Pu, L. The first dendrimer-based enantioselective fluorescent sensor for the recognition of chiral amino alcohols. *Angew. Chem.* **2000**, *112*, 3784–3787. [[CrossRef](#)]
55. Pu, L. Enantioselective fluorescent sensors: A tale of BINOL. *Acc. Chem. Res.* **2012**, *45*, 150–163. [[CrossRef](#)] [[PubMed](#)]
56. Wanderley, M.M.; Wang, C.; Wu, C.-D.; Lin, W. A chiral porous metal–organic framework for highly sensitive and enantioselective fluorescence sensing of amino alcohols. *J. Am. Chem. Soc.* **2012**, *134*, 9050–9053. [[CrossRef](#)]
57. Chandrasekhar, P.; Mukhopadhyay, A.; Savitha, G.; Moorthy, J.N. Remarkably selective and enantiodifferentiating sensing of histidine by a fluorescent homochiral Zn-MOF based on pyrene-tetralactic acid. *Chem. Sci.* **2016**, *7*, 3085–3091. [[CrossRef](#)]
58. Zhao, X.; Nguyen, E.T.; Hong, A.N.; Feng, P.; Bu, X. Chiral isocamphoric acid: Founding a large family of homochiral porous materials. *Angew. Chem. Int. Ed.* **2018**, *57*, 7101–7105. [[CrossRef](#)]
59. Han, Z.; Wang, K.; Guo, Y.; Chen, W.; Zhang, J.; Zhang, X.; Siligardi, G.; Yang, S.; Zhou, Z.; Sun, P. Cation-induced chirality in a bifunctional metal-organic framework for quantitative enantioselective recognition. *Nat. Commun.* **2019**, *10*, 5117. [[CrossRef](#)]

60. Li, S.; Zhou, Y.; Yan, B. Zirconium Metal Organic Framework-Based Hybrid Sensors with Chiral and Luminescent Centers Fabricated by Postsynthetic Modification for the Detection and Recognition of Tryptophan Enantiomers. *Inorg. Chem.* **2022**, *61*, 9615–9622. [[CrossRef](#)]
61. Guo, D.; Zhou, X.; Huang, S.; Zhu, Y. Enantioselective fluorescent detection of lysine enantiomers by functionalized achiral metal organic frameworks. *Microchem. J.* **2022**, *181*, 107666. [[CrossRef](#)]
62. Freedman, T.B.; Cao, X.; Dukor, R.K.; Nafie, L.A. Absolute configuration determination of chiral molecules in the solution state using vibrational circular dichroism. *Chirality* **2003**, *15*, 743–758. [[CrossRef](#)] [[PubMed](#)]
63. Zhang, X.; Yin, J.; Yoon, J. Recent advances in development of chiral fluorescent and colorimetric sensors. *Chem. Rev.* **2014**, *114*, 4918–4959. [[CrossRef](#)] [[PubMed](#)]
64. Neidig, M.L.; Weckler, A.T.; Schenk, G.; Holman, T.R.; Solomon, E.I. Kinetic and spectroscopic studies of N694C lipoxygenase: A probe of the substrate activation mechanism of a nonheme ferric enzyme. *J. Am. Chem. Soc.* **2007**, *129*, 7531–7537. [[CrossRef](#)] [[PubMed](#)]
65. Schreiber, R.; Luong, N.; Fan, Z.; Kuzyk, A.; Nickels, P.C.; Zhang, T.; Smith, D.M.; Yurke, B.; Kuang, W.; Govorov, A.O. Chiral plasmonic DNA nanostructures with switchable circular dichroism. *Nat. Commun.* **2013**, *4*, 2948. [[CrossRef](#)] [[PubMed](#)]
66. Berova, N.; Di Bari, L.; Pescitelli, G. Application of electronic circular dichroism in configurational and conformational analysis of organic compounds. *Chem. Soc. Rev.* **2007**, *36*, 914–931. [[CrossRef](#)]
67. Wang, F.; Tang, Y.-H.; Zhang, J. Achievement of bulky homochirality in zeolitic imidazolate-related frameworks. *Inorg. Chem.* **2015**, *54*, 11064–11066. [[CrossRef](#)]
68. Li, M.-Y.; Wang, F.; Gu, Z.-G.; Zhang, J. Synthesis of homochiral zeolitic metal–organic frameworks with amino acid and tetrazolates for chiral recognition. *RSC Adv.* **2017**, *7*, 4872–4875. [[CrossRef](#)]
69. Zhao, Y.-W.; Wang, Y.; Zhang, X.-M. Homochiral MOF as circular dichroism sensor for enantioselective recognition on nature and chirality of unmodified amino acids. *ACS Appl. Mater. Interfaces* **2017**, *9*, 20991–20999. [[CrossRef](#)]
70. Yao, R.-X.; Fu, H.-H.; Yu, B.; Zhang, X.-M. Chiral metal–organic frameworks constructed from four-fold helical chain SBUs for enantioselective recognition of α -hydroxy/amino acids. *Inorg. Chem. Front.* **2018**, *5*, 153–159. [[CrossRef](#)]
71. Zhu, Y.; Zhou, Y.; Zhang, X.; Sun, Z.; Jiao, C. Homochiral MOF as Chiroptical Sensor for Determination of Absolute Configuration and Enantiomeric Ratio of Chiral Tryptophan. *Adv. Opt. Mater.* **2021**, *9*, 2001889. [[CrossRef](#)]
72. Duan, H.-J.; Yang, C.-X.; Yan, X.-P. Chiral metal–organic framework coated quartz crystal microbalance for chiral discrimination. *RSC Adv.* **2015**, *5*, 30577–30582. [[CrossRef](#)]
73. Liu, B.; Shekhah, O.; Arslan, H.K.; Liu, J.; Wöll, C.; Fischer, R.A. Enantiopure metal–organic framework thin films: Oriented SURMOF growth and enantioselective adsorption. *Angew. Chem. Int. Ed.* **2012**, *51*, 807–810. [[CrossRef](#)] [[PubMed](#)]
74. Xiao, Y.-H.; Gu, Z.-G.; Zhang, J. Surface-coordinated metal–organic framework thin films (SURMOFs) for electrocatalytic applications. *Nanoscale* **2020**, *12*, 12712–12730. [[CrossRef](#)] [[PubMed](#)]
75. Chen, S.-M.; Chang, L.-M.; Yang, X.-K.; Luo, T.; Xu, H.; Gu, Z.-G.; Zhang, J. Liquid-Phase Epitaxial Growth of Azapyrene-Based Chiral Metal–Organic Framework Thin Films for Circularly Polarized Luminescence. *ACS Appl. Mater. Interfaces* **2019**, *11*, 31421–31426. [[CrossRef](#)] [[PubMed](#)]
76. Cakici, M.; Gu, Z.-G.; Nieger, M.; Bürck, J.; Heinke, L.; Bräse, S. Planar-chiral building blocks for metal–organic frameworks. *Chem. Commun.* **2015**, *51*, 4796–4798. [[CrossRef](#)] [[PubMed](#)]
77. Yang, X.-L.; Zang, R.-B.; Shao, R.; Guan, R.-F.; Xie, M.-H. Chiral UiO-MOFs based QCM sensors for enantioselective discrimination of hazardous biomolecule. *J. Hazard. Mater.* **2021**, *413*, 125467. [[CrossRef](#)]
78. Okur, S.; Qin, P.; Chandresh, A.; Li, C.; Zhang, Z.; Lemmer, U.; Heinke, L. An enantioselective e-nose: An array of nanoporous homochiral MOF films for stereospecific sensing of chiral odors. *Angew. Chem. Int. Ed.* **2021**, *60*, 3566–3571. [[CrossRef](#)]
79. Hassanpour, S.; Baradaran, B.; Hejazi, M.; Hasanzadeh, M.; Mokhtarzadeh, A.; de la Guardia, M. Recent trends in rapid detection of influenza infections by bio and nanobiosensor. *TrAC Trends Anal. Chem.* **2018**, *98*, 201–215. [[CrossRef](#)]
80. Zhu, G.; Kingsford, O.J.; Yi, Y.; Wong, K.-y. Recent advances in electrochemical chiral recognition. *J. Electrochem. Soc.* **2019**, *166*, H205. [[CrossRef](#)]
81. Liu, W.; Yin, X.-B. Metal–organic frameworks for electrochemical applications. *TrAC Trends Anal. Chem.* **2016**, *75*, 86–96. [[CrossRef](#)]
82. Wang, C.; Liu, X.; Demir, N.K.; Chen, J.P.; Li, K. Applications of water stable metal–organic frameworks. *Chem. Soc. Rev.* **2016**, *45*, 5107–5134. [[CrossRef](#)] [[PubMed](#)]
83. Zhao, F.; Sun, T.; Geng, F.; Chen, P.; Gao, Y. Metal-organic frameworks-based electrochemical sensors and biosensors. *Int. J. Electrochem. Sci.* **2019**, *14*, 5287–5304. [[CrossRef](#)]
84. Chuang, C.H.; Kung, C.W. Metal–Organic frameworks toward electrochemical sensors: Challenges and opportunities. *Electroanalysis* **2020**, *32*, 1885–1895. [[CrossRef](#)]
85. Kuang, R.; Zheng, L.; Chi, Y.; Shi, J.; Chen, X.; Zhang, C. Highly efficient electrochemical recognition and quantification of amine enantiomers based on a guest-free homochiral MOF. *RSC Adv.* **2017**, *7*, 11701–11706. [[CrossRef](#)]
86. Wu, T.; Wei, X.; Ma, X.; Li, J. Amperometric sensing of L-phenylalanine using a gold electrode modified with a metal organic framework, a molecularly imprinted polymer, and β -cyclodextrin-functionalized gold nanoparticles. *Microchim. Acta* **2017**, *184*, 2901–2907. [[CrossRef](#)]
87. Wei, X.; Li, L.; Lian, H.; Cao, X.; Liu, B. Grain-like chiral metal-organic framework/multi-walled carbon nanotube composited electroensing interface for enantioselective recognition of Tryptophan. *J. Electroanal. Chem.* **2021**, *886*, 115108. [[CrossRef](#)]

88. Hou, Y.; Liang, J.; Kuang, X.; Kuang, R. Simultaneous electrochemical recognition of tryptophan and penicillamine enantiomers based on MOF-modified β -CD. *Carbohydr. Polym.* **2022**, *290*, 119474. [[CrossRef](#)]
89. Li, H.; Wang, L.; Yan, S.; Chen, J.; Zhang, M.; Zhao, R.; Niu, X.; Wang, K. Fusiform-like metal-organic framework for enantioselective discrimination of tryptophan enantiomers. *Electrochim. Acta* **2022**, *419*, 140409. [[CrossRef](#)]
90. Niu, X.; Yan, S.; Chen, J.; Li, H.; Wang, K. Enantioselective recognition of L/D-amino acids in the chiral nanochannels of a metal-organic framework. *Electrochim. Acta* **2022**, *405*, 139809. [[CrossRef](#)]
91. Liu, N.; Yang, B.; Yin, Z.-Z.; Cai, W.; Li, J.; Kong, Y. A chiral sensing platform based on chiral metal-organic framework for enantiodiscrimination of the isomers of tyrosine and tryptophan. *J. Electroanal. Chem.* **2022**, *918*, 116445. [[CrossRef](#)]
92. Long, Z.; Jia, J.; Wang, S.; Kou, L.; Hou, X.; Sepaniak, M.J. Visual enantioselective probe based on metal organic framework incorporating quantum dots. *Microchem. J.* **2013**, *110*, 764–769. [[CrossRef](#)]
93. Zhang, Q.; Lei, M.; Kong, F.; Yang, Y. A water-stable homochiral luminescent MOF constructed from an achiral acylamide-containing dicarboxylate ligand for enantioselective sensing of penicillamine. *Chem. Commun.* **2018**, *54*, 10901–10904. [[CrossRef](#)] [[PubMed](#)]
94. Han, Z.; Wang, K.; Min, H.; Xu, J.; Shi, W.; Cheng, P. Bifunctionalized Metal–Organic Frameworks for Pore-Size-Dependent Enantioselective Sensing. *Angew. Chem. Int. Ed.* **2022**, *61*, e202204066. [[CrossRef](#)] [[PubMed](#)]
95. Liu, Y.; Liu, L.; Chen, X.; Liu, Y.; Han, Y.; Cui, Y. Single-crystalline ultrathin 2D porous nanosheets of chiral metal–organic frameworks. *J. Am. Chem. Soc.* **2021**, *143*, 3509–3518. [[CrossRef](#)]
96. Tan, C.; Yang, K.; Dong, J.; Liu, Y.; Liu, Y.; Jiang, J.; Cui, Y. Boosting enantioselectivity of chiral organocatalysts with ultrathin two-dimensional metal–organic framework nanosheets. *J. Am. Chem. Soc.* **2019**, *141*, 17685–17695. [[CrossRef](#)]
97. Xiao, J.; Wang, X.; Xu, X.; Tian, F.; Liu, Z. Fabrication of a “turn-on”-type enantioselective fluorescence sensor via a modified achiral MOF: Applications for synchronous detection of phenylalaninol enantiomers. *Analyst* **2021**, *146*, 937–942. [[CrossRef](#)]
98. Kuang, X.; Ye, S.; Li, X.; Ma, Y.; Zhang, C.; Tang, B. A new type of surface-enhanced Raman scattering sensor for the enantioselective recognition of D/L-cysteine and D/L-asparagine based on a helically arranged Ag NPs@ homochiral MOF. *Chem. Commun.* **2016**, *52*, 5432–5435. [[CrossRef](#)]
99. Zhao, Y.-W.; Guo, L.-E.; Zhang, F.-Q.; Yao, J.; Zhang, X.-M. Turn-On Fluorescence Enantioselective Sensing of Hydroxyl Carboxylic Enantiomers by Metal–Organic Framework Nanosheets with a Homochiral Tetracarboxylate of Cyclohexane Diamide. *ACS Appl. Mater. Interfaces* **2021**, *13*, 20821–20829. [[CrossRef](#)]
100. Kuang, X.; Ma, Y.; Zhang, C.; Su, H.; Zhang, J.; Tang, B. A new synthesis strategy for chiral CdS nanotubes based on a homochiral MOF template. *Chem. Commun.* **2015**, *51*, 5955–5958. [[CrossRef](#)]
101. Shili, Q.; Yangyang, S.; Xudong, H.; Hongtao, C.; Lidi, G.; Zhongyu, H.; Dongsheng, Z.; Xinyao, L.; Sibing, Z. Chiral fluorescence recognition of glutamine enantiomers by a modified Zr-based MOF based on solvent-assisted ligand incorporation. *RSC Adv.* **2021**, *11*, 37584–37594. [[CrossRef](#)]
102. Zhu, S.; Lin, X.; Ran, P.; Xia, Q.; Yang, C.; Ma, J.; Fu, Y. A novel luminescence-functionalized metal-organic framework nanoflowers electrochemiluminescence sensor via “on-off” system. *Biosens. Bioelectron.* **2017**, *91*, 436–440. [[CrossRef](#)] [[PubMed](#)]
103. Deng, C.-H.; Li, T.; Chen, J.-H.; Ma, J.-G.; Cheng, P. The electrochemical discrimination of pinene enantiomers by a cyclodextrin metal–organic framework. *Dalton Trans.* **2017**, *46*, 6830–6834. [[CrossRef](#)] [[PubMed](#)]
104. Hou, Y.; Liu, Z.; Tong, L.; Zhao, L.; Kuang, X.; Kuang, R.; Ju, H. One-step electrodeposition of the MOF@ CCQDs/NiF electrode for chiral recognition of tyrosine isomers. *Dalton Trans.* **2020**, *49*, 31–34. [[CrossRef](#)] [[PubMed](#)]
105. Zhao, L.; Kuang, X.; Kuang, R.; Tong, L.; Liu, Z.; Hou, Y.; Sun, X.; Wang, Z.; Wei, Q. MOF-based supramolecule helical nanomaterials: Toward highly enantioselective electrochemical recognition of penicillamine. *ACS Appl. Mater. Interfaces* **2019**, *12*, 1533–1538. [[CrossRef](#)] [[PubMed](#)]
106. Zhou, S.; Guo, J.; Dai, Z.; Liu, C.; Zhao, J.; Gao, Z.; Song, Y.-Y. Engineering homochiral MOFs in TiO₂ nanotubes as enantioselective photoelectrochemical electrode for chiral recognition. *Anal. Chem.* **2021**, *93*, 12067–12074. [[CrossRef](#)] [[PubMed](#)]
107. Zhang, L.; Qiao, C.; Cai, X.; Xia, Z.; Han, J.; Yang, Q.; Zhou, C.; Chen, S.; Gao, S. Microcalorimetry-guided pore-microenvironment optimization to improve sensitivity of Ni-MOF electrochemical biosensor for chiral galantamine. *Chem. Eng. J.* **2021**, *426*, 130730. [[CrossRef](#)]
108. Liu, Z.; Kuang, X.; Sun, X.; Zhang, Y.; Wei, Q. Electrochemical enantioselective recognition penicillamine isomers based on chiral C-dots/MOF hybrid arrays. *J. Electroanal. Chem.* **2019**, *846*, 113151. [[CrossRef](#)]
109. Wei, X.; Chen, Y.; He, S.; Lian, H.; Cao, X.; Liu, B. L-histidine-regulated zeolitic imidazolate framework modified electrochemical interface for enantioselective determination of L-glutamate. *Electrochim. Acta* **2021**, *400*, 139464. [[CrossRef](#)]
110. Wu, X.-Q.; Feng, P.-Q.; Guo, Z.; Wei, X. Water-sTable 1D double-chain Cu metal–organic framework-based electrochemical biosensor for detecting l-tyrosine. *Langmuir* **2020**, *36*, 14123–14129. [[CrossRef](#)]
111. Tistaert, C.; Dejaegher, B.; Vander Heyden, Y. Chromatographic separation techniques and data handling methods for herbal fingerprints: A review. *Anal. Chim. Acta* **2011**, *690*, 148–161. [[CrossRef](#)]
112. Li, X.; Chang, C.; Wang, X.; Bai, Y.; Liu, H. Applications of homochiral metal-organic frameworks in enantioselective adsorption and chromatography separation. *Electrophoresis* **2014**, *35*, 2733–2743. [[CrossRef](#)] [[PubMed](#)]
113. Gu, Z.-Y.; Yang, C.-X.; Chang, N.; Yan, X.-P. Metal–organic frameworks for analytical chemistry: From sample collection to chromatographic separation. *Acc. Chem. Res.* **2012**, *45*, 734–745. [[CrossRef](#)] [[PubMed](#)]

114. Corella-Ochoa, M.N.; Tapia, J.B.; Rubin, H.N.; Lillo, V.; González-Cobos, J.; Núñez-Rico, J.L.; Balestra, S.R.; Almora-Barrios, N.; Lledós, M.; Güell-Bara, A. Homochiral metal–organic frameworks for enantioselective separations in liquid chromatography. *J. Am. Chem. Soc.* **2019**, *141*, 14306–14316. [[CrossRef](#)] [[PubMed](#)]
115. Firooz, S.K.; Armstrong, D.W. Metal-organic frameworks in separations: A review. *Anal. Chim. Acta* **2022**, *1234*, 340208. [[CrossRef](#)]
116. Si, T.; Lu, X.; Zhang, H.; Wang, S.; Liang, X.; Guo, Y. Metal-organic framework-based core-shell composites for chromatographic stationary phases. *TrAC Trends Anal. Chem.* **2022**, *149*, 116545. [[CrossRef](#)]
117. Nuzhdin, A.L.; Dybtsev, D.N.; Bryliakov, K.P.; Talsi, E.P.; Fedin, V.P. Enantioselective chromatographic resolution and one-pot synthesis of enantiomerically pure sulfoxides over a homochiral Zn-organic framework. *J. Am. Chem. Soc.* **2007**, *129*, 12958–12959. [[CrossRef](#)]
118. Tanaka, K.; Muraoka, T.; Hirayama, D.; Ohnishi, A. Highly efficient chromatographic resolution of sulfoxides using a new homochiral MOF–silica composite. *Chem. Commun.* **2012**, *48*, 8577–8579. [[CrossRef](#)]
119. Kuang, X.; Ma, Y.; Su, H.; Zhang, J.; Dong, Y.-B.; Tang, B. High-performance liquid chromatographic enantioseparation of racemic drugs based on homochiral metal–organic framework. *Anal. Chem.* **2014**, *86*, 1277–1281. [[CrossRef](#)]
120. Hartlieb, K.J.; Holcroft, J.M.; Moghadam, P.Z.; Vermeulen, N.A.; Algaradah, M.M.; Nassar, M.S.; Botros, Y.Y.; Snurr, R.Q.; Stoddart, J.F. CD-MOF: A versatile separation medium. *J. Am. Chem. Soc.* **2016**, *138*, 2292–2301. [[CrossRef](#)]
121. Wang, C.; Zhang, L.; Li, X.; Yu, A.; Zhang, S. Controlled fabrication of core-shell silica@chiral metal-organic framework for significant improvement chromatographic separation of enantiomers. *Talanta* **2020**, *218*, 121155. [[CrossRef](#)]
122. Yu, Y.; Xu, N.; Zhang, J.; Wang, B.; Xie, S.; Yuan, L. Chiral metal–organic framework d-His-ZIF-8@SiO₂ core-shell microspheres used for HPLC enantioseparations. *ACS Appl. Mater. Interfaces* **2020**, *12*, 16903–16911. [[CrossRef](#)] [[PubMed](#)]
123. Jiang, H.; Yang, K.; Zhao, X.; Zhang, W.; Liu, Y.; Jiang, J.; Cui, Y. Highly stable Zr (IV)-based metal–organic frameworks for chiral separation in reversed-phase liquid chromatography. *J. Am. Chem. Soc.* **2020**, *143*, 390–398. [[CrossRef](#)]
124. Chen, J.-K.; Yu, Y.-Y.; Xu, N.-Y.; Guo, P.; Zhang, J.-H.; Wang, B.-J.; Xie, S.-M.; Yuan, L.-M. Chiral polyaniline modified Metal-Organic framework Core-Shell composite MIL-101@c-PANI for HPLC enantioseparation. *Microchem. J.* **2021**, *169*, 106576. [[CrossRef](#)]
125. Ma, X.; Guo, Y.; Zhang, L.; Wang, K.; Yu, A.; Zhang, S.; Ouyang, G. Crystal morphology tuning and green post-synthetic modification of metal organic framework for HPLC enantioseparation. *Talanta* **2022**, *239*, 123143. [[CrossRef](#)] [[PubMed](#)]
126. Tanaka, K.; Muraoka, T.; Otubo, Y.; Takahashi, H.; Ohnishi, A. HPLC enantioseparation on a homochiral MOF–silica composite as a novel chiral stationary phase. *RSC Adv.* **2016**, *6*, 21293–21301. [[CrossRef](#)]
127. Zhang, M.; Chen, X.; Zhang, J.; Kong, J.; Yuan, L. A 3D Homochiral MOF [Cd₂(d-cam)₃]•2H₂O•4dma for HPLC Chromatographic Enantioseparation. *Chirality* **2016**, *28*, 340–346. [[CrossRef](#)]
128. Yuan, B.; Li, L.; Yu, Y.; Xu, N.; Fu, N.; Zhang, J.; Zhang, M.; Wang, B.; Xie, S.; Yuan, L. Chiral metal-organic framework [Co₂(D-cam)₂(TMDPy)]@SiO₂ core-shell microspheres for HPLC separation. *Microchem. J.* **2021**, *161*, 105815. [[CrossRef](#)]
129. Zhang, M.; Pu, Z.-J.; Chen, X.-L.; Gong, X.-L.; Zhu, A.-X.; Yuan, L.-M. Chiral recognition of a 3D chiral nanoporous metal–organic framework. *Chem. Commun.* **2013**, *49*, 5201–5203. [[CrossRef](#)]
130. Tanaka, K.; Hotta, N.; Nagase, S.; Yoza, K. Efficient HPLC enantiomer separation using a pillared homochiral metal–organic framework as a novel chiral stationary phase. *New J. Chem.* **2016**, *40*, 4891–4894. [[CrossRef](#)]
131. Zhang, M.; Xue, X.-D.; Zhang, J.-H.; Xie, S.-M.; Zhang, Y.; Yuan, L.-M. Enantioselective chromatographic resolution using a homochiral metal–organic framework in HPLC. *Anal. Methods* **2014**, *6*, 341–346. [[CrossRef](#)]
132. Hailili, R.; Wang, L.; Qv, J.; Yao, R.; Zhang, X.-M.; Liu, H. Planar Mn₄O cluster homochiral metal–organic framework for HPLC separation of pharmaceutically important (±)-ibuprofen racemate. *Inorg. Chem.* **2015**, *54*, 3713–3715. [[CrossRef](#)] [[PubMed](#)]
133. Xie, S.; Hu, C.; Li, L.; Zhang, J.; Fu, N.; Wang, B.; Yuan, L. Homochiral metal-organic framework for HPLC separation of enantiomers. *Microchem. J.* **2018**, *139*, 487–491. [[CrossRef](#)]
134. Yang, C.-X.; Zheng, Y.-Z.; Yan, X.-P. γ -Cyclodextrin metal–organic framework for efficient separation of chiral aromatic alcohols. *RSC Adv.* **2017**, *7*, 36297–36301. [[CrossRef](#)]
135. Zhang, J.H.; Nong, R.Y.; Xie, S.M.; Wang, B.J.; Ai, P.; Yuan, L.M. Homochiral metal-organic frameworks based on amino acid ligands for HPLC separation of enantiomers. *Electrophoresis* **2017**, *38*, 2513–2520. [[CrossRef](#)]
136. Zhang, M.; Zhang, J.-H.; Zhang, Y.; Wang, B.-J.; Xie, S.-M.; Yuan, L.-M. Chromatographic study on the high performance separation ability of a homochiral [Cu₂(d-Cam)₂(4,4'-bpy)]_n based-column by using racemates and positional isomers as test probes. *J. Chromatogr. A* **2014**, *1325*, 163–170. [[CrossRef](#)]
137. Zhang, P.; Wang, L.; Zhang, J.-H.; He, Y.-J.; Li, Q.; Luo, L.; Zhang, M.; Yuan, L.-M. Homochiral metal-organic framework immobilized on silica gel by the interfacial polymerization for HPLC enantioseparations. *J. Liq. Chromatogr. Relat. Technol.* **2018**, *41*, 903–909. [[CrossRef](#)]
138. Yu, Y.; Yuan, B.; Hu, C.; Fu, N.; Xu, N.; Zhang, J.; Wang, B.; Xie, S.; Yuan, L. Homochiral Metal–Organic Framework [Co(L)(bpe)₂(H₂O)₂]. H₂O Used for Separation of Racemates in High-Performance Liquid Chromatography. *J. Chromatogr. Sci.* **2021**, *59*, 355–360. [[CrossRef](#)]
139. Chen, J.K.; Xu, N.Y.; Guo, P.; Wang, B.J.; Zhang, J.H.; Xie, S.M.; Yuan, L.M. A chiral metal-organic framework core-shell microspheres composite for high-performance liquid chromatography enantioseparation. *J. Sep. Sci.* **2021**, *44*, 3976–3985. [[CrossRef](#)]

140. Xu, N.; Yuan, B.; Hu, C.; Yu, Y.; Fu, N.; Zhang, J.; Xie, S.; Yuan, L. Homochiral Metal–Organic Framework [Ni (S-mal)(bpy)]_n Used for the Separation of Racemic Compounds by High Performance Liquid Chromatography. *J. Anal. Chem.* **2021**, *76*, 749–754. [[CrossRef](#)]
141. Menezes, T.; Santos, K.; Franceschi, E.; Borges, G.; Dariva, C.; Egues, S.; De Conto, J.; Santana, C. Synthesis of the chiral stationary phase based on functionalized ZIF-8 with amylose carbamate. *J. Mater. Res.* **2020**, *35*, 2936–2949. [[CrossRef](#)]
142. Yohannes, A.; Feng, X.; Yao, S. Dispersive solid-phase extraction of racemic drugs using chiral ionic liquid-metal-organic framework composite sorbent. *J. Chromatogr. A* **2020**, *1627*, 461395. [[CrossRef](#)] [[PubMed](#)]
143. Wang, X.; Zhang, J.; Yu, A.; Zhang, S.; Hu, G.; Ouyang, G. Experimentally probing the chiral recognition mechanism of 1, 1'-bi-2-naphthol on a nitrogen enriched chiral metal-organic framework. *Microchem. J.* **2022**, *174*, 107092. [[CrossRef](#)]
144. Ma, X.; Zhou, X.; Yu, A.; Zhao, W.; Zhang, W.; Zhang, S.; Wei, L.; Cook, D.J.; Roy, A. Functionalized metal-organic framework nanocomposites for dispersive solid phase extraction and enantioselective capture of chiral drug intermediates. *J. Chromatogr. A* **2018**, *1537*, 1–9. [[CrossRef](#)] [[PubMed](#)]
145. Choi, H.-J.; Koh, D.-Y. Homochiral Metal-Organic Framework Based Mixed Matrix Membrane for Chiral Resolution. *Membranes* **2022**, *12*, 357. [[CrossRef](#)] [[PubMed](#)]
146. Xie, S.-M.; Zhang, Z.-J.; Wang, Z.-Y.; Yuan, L.-M. Chiral metal–organic frameworks for high-resolution gas chromatographic separations. *J. Am. Chem. Soc.* **2011**, *133*, 11892–11895. [[CrossRef](#)]
147. Tang, W.Q.; Xu, J.Y.; Gu, Z.Y. Metal–organic-framework-based gas chromatographic separation. *Chem.–Asian J.* **2019**, *14*, 3462–3473. [[CrossRef](#)]
148. Xie, S.-m.; Zhang, X.-h.; Wang, B.-j.; Zhang, M.; Zhang, J.-h.; Yuan, L.-m. 3D Chiral nanoporous metal–organic framework for chromatographic separation in GC. *Chromatographia* **2014**, *77*, 1359–1365. [[CrossRef](#)]
149. Yang, J.-r.; Xie, S.-m.; Zhang, J.-h.; Chen, L.; Nong, R.-y.; Yuan, L.-m. Metal–organic framework [Cd (LTP) 2]_n for improved enantioseparations on a chiral cyclodextrin stationary phase in GC. *J. Chromatogr. Sci.* **2017**, *54*, 1467–1474. [[CrossRef](#)]
150. Xie, S.-M.; Zhang, X.-H.; Zhang, Z.-J.; Zhang, M.; Jia, J.; Yuan, L.-M. A 3-D open-framework material with intrinsic chiral topology used as a stationary phase in gas chromatography. *Anal. Bioanal. Chem.* **2013**, *405*, 3407–3412. [[CrossRef](#)]
151. Xie, S.; Wang, B.; Zhang, X.; Zhang, J.; Zhang, M.; Yuan, L. Chiral 3D open-framework material Ni (D-cam)(H₂O)₂ used as GC stationary phase. *Chirality* **2014**, *26*, 27–32. [[CrossRef](#)]
152. Xie, S.-M.; Zhang, X.-H.; Zhang, Z.-J.; Yuan, L.-M. Porous chiral metal-organic framework InH (D-C10H14O₄)₂ with anionic-type diamond network for high-resolution gas chromatographic enantioseparations. *Anal. Lett.* **2013**, *46*, 753–763. [[CrossRef](#)]
153. Zhang, X.-h.; Xie, S.-m.; Duan, A.-h.; Wang, B.-j.; Yuan, L.-M. Separation performance of MOFs Zn (ISN) 2· 2H₂O as stationary phase for high-resolution GC. *Chromatographia* **2013**, *76*, 831–836. [[CrossRef](#)]
154. Yang, J.-r.; Xie, S.-m.; Liu, H.; Zhang, J.-h.; Yuan, L.-m. Metal–Organic Framework InH (d-C10H14O₄)₂ for Improved Enantioseparations on a Chiral Cyclodextrin Stationary Phase in GC. *Chromatographia* **2015**, *78*, 557–564. [[CrossRef](#)]
155. Liu, H.; Xie, S.M.; Ai, P.; Zhang, J.H.; Zhang, M.; Yuan, L.M. Metal–Organic Framework Co (d-Cam) 1/2 (bdc) 1/2 (tmdpy) for Improved Enantioseparations on a Chiral Cyclodextrin Stationary Phase in Gas Chromatography. *ChemPlusChem* **2014**, *79*, 1103–1108. [[CrossRef](#)]
156. Kou, W.-T.; Yang, C.-X.; Yan, X.-P. Post-synthetic modification of metal–organic frameworks for chiral gas chromatography. *J. Mater. Chem. A* **2018**, *6*, 17861–17866. [[CrossRef](#)]
157. Fanali, S.; Catarcini, P.; Blaschke, G.; Chankvetadze, B. Enantioseparations by capillary electrochromatography. *Electrophoresis* **2001**, *22*, 3131–3151. [[CrossRef](#)]
158. Fei, Z.-X.; Zhang, M.; Zhang, J.-H.; Yuan, L.-M. Chiral metal–organic framework used as stationary phases for capillary electrochromatography. *Anal. Chim. Acta* **2014**, *830*, 49–55. [[CrossRef](#)]
159. Ye, N.; Ma, J.; An, J.; Li, J.; Cai, Z.; Zong, H. Separation of amino acid enantiomers by a capillary modified with a metal–organic framework. *RSC Adv.* **2016**, *6*, 41587–41593. [[CrossRef](#)]
160. Ding, W.; Yu, T.; Du, Y.; Sun, X.; Feng, Z.; Zhao, S.; Ma, X.; Ma, M.; Chen, C. A metal organic framework-functionalized monolithic column for enantioseparation of six basic chiral drugs by capillary electrochromatography. *Microchim. Acta* **2020**, *187*, 51. [[CrossRef](#)]
161. Sun, X.; Niu, B.; Zhang, Q.; Chen, Q. MIL-53-based homochiral metal–organic framework as a stationary phase for open-tubular capillary electrochromatography. *J. Pharm. Anal.* **2022**, *12*, 509–516. [[CrossRef](#)]
162. Lidi, G.; Xingfang, H.; Shili, Q.; Hongtao, C.; Xuan, Z.; Bingbing, W. l-Cysteine modified metal–organic framework as a chiral stationary phase for enantioseparation by capillary electrochromatography. *RSC Adv.* **2022**, *12*, 6063–6075. [[CrossRef](#)] [[PubMed](#)]
163. Wang, C.; Zhu, D.; Zhang, J.; Du, Y. Homochiral iron-based γ -cyclodextrin metal-organic framework for stereoisomer separation in the open tubular capillary electrochromatography. *J. Pharm. Biomed. Anal.* **2022**, *215*, 114777. [[CrossRef](#)] [[PubMed](#)]
164. Wang, C.; Chen, C.; Ma, M.; Feng, Z.; Du, Y. In-situ grown metal organic framework synergistic system for the enantioseparation of three drugs in open tubular capillary electrochromatography. *J. Sep. Sci.* **2022**, *45*, 2708–2716. [[CrossRef](#)] [[PubMed](#)]
165. Miao, P.; Zhang, L.; Zhang, J.; Ma, M.; Du, Y.; Gan, J.; Yang, J. Metal organic framework-modified monolithic column immobilized with pepsin for enantioseparation in capillary electrochromatography. *J. Chromatogr. B* **2022**, *1203*, 123306. [[CrossRef](#)] [[PubMed](#)]
166. Gao, L.; Hu, X.; Qin, S.; Chu, H.; Tang, Y.; Li, X.; Wang, B. One-pot synthesis of a novel chiral Zr-based metal-organic framework for capillary electrochromatographic enantioseparation. *Electrophoresis* **2022**, *43*, 1161–1173. [[CrossRef](#)] [[PubMed](#)]

167. Fei, Z.X.; Zhang, M.; Xie, S.M.; Yuan, L.M. Capillary electrochromatographic fast enantioseparation based on a chiral metal–organic framework. *Electrophoresis* **2014**, *35*, 3541–3548. [[CrossRef](#)]
168. Sun, X.; Tao, Y.; Du, Y.; Ding, W.; Chen, C.; Ma, X. Metal organic framework HKUST-1 modified with carboxymethyl- β -cyclodextrin for use in improved open tubular capillary electrochromatographic enantioseparation of five basic drugs. *Microchim. Acta* **2019**, *186*, 462. [[CrossRef](#)]
169. Pan, C.; Lv, W.; Niu, X.; Wang, G.; Chen, H.; Chen, X. Homochiral zeolite-like metal-organic framework with DNA like double-helicity structure as stationary phase for capillary electrochromatography enantioseparation. *J. Chromatogr. A* **2018**, *1541*, 31–38. [[CrossRef](#)]
170. Ding, W.; Ma, M.; Du, Y.; Chen, C.; Ma, X. Metal organic framework ZIF-90 modified with lactobionic acid for use in improved open tubular capillary electrochromatographic enantioseparation of five basic drugs. *Microchim. Acta* **2020**, *187*, 651. [[CrossRef](#)]
171. Ma, J.; Ye, N.; Li, J. Covalent bonding of homochiral metal-organic framework in capillaries for stereoisomer separation by capillary electrochromatography. *Electrophoresis* **2016**, *37*, 601–608. [[CrossRef](#)]
172. Pan, C.; Wang, W.; Zhang, H.; Xu, L.; Chen, X. In situ synthesis of homochiral metal–organic framework in capillary column for capillary electrochromatography enantioseparation. *J. Chromatogr. A* **2015**, *1388*, 207–216. [[CrossRef](#)] [[PubMed](#)]
173. Li, Z.; Mao, Z.; Zhou, W.; Chen, Z. γ -Cyclodextrin metal-organic framework supported by polydopamine as stationary phases for electrochromatographic enantioseparation. *Talanta* **2020**, *218*, 121160. [[CrossRef](#)] [[PubMed](#)]
174. Wang, T.; Wang, Y.; Zhang, Y.; Cheng, Y.; Ye, J.; Chu, Q.; Cheng, G. Rapid preparation and evaluation of chiral open-tubular columns supported with bovine serum album and zeolite imidazolate framework-8 for mini-capillary electrochromatography. *J. Chromatogr. A* **2020**, *1625*, 461284. [[CrossRef](#)] [[PubMed](#)]

Disclaimer/Publisher’s Note: The statements, opinions and data contained in all publications are solely those of the individual author(s) and contributor(s) and not of MDPI and/or the editor(s). MDPI and/or the editor(s) disclaim responsibility for any injury to people or property resulting from any ideas, methods, instructions or products referred to in the content.